ABSTRACT

This document describes the algorithmic and theoretic basis of the lunar irradiance model. It includes the method to adjust the model based on irradiance measurements. It also describes how to propagate the uncertainties throughout the entire model chain.

Adriaensen Stefan(1) Taylor Sarah (2)

VITO (1), NPL (2)

31 March 2021

LUNAR IRRADIANCE MODEL ALGORITHM AND THEORETICAL BASIS DOCUMENT

Delivery 7

This document was produced as part of the ESA-funded project “Lunar spectral irradiance measurement and modelling for absolute calibration of EO optical sensors” under ESA contract number: 4000121576/17/NL/AF/hh

esa NPL National Physical Laboratory vito Universidad de Valladolid

1.1.1.1.1 Signatures and version history

1.1.1.1.2

	Name	Organisation	Date
Written by	Stefan Adriaensen	VITO	26-Feb-2018
Reviewed by (consortium)	Emma Woolliams	NPL	9-Dec-2019
Approved by (ESA)	Marc Bouvet	ESA	12-Dec-2019

1.1.1.1.3 Version history

Version	Date	Publicly available or private to consortium?
0.1	19/03/2018	created
0.2	28/02/2019	Add description model regression and rearrange the document
0.3	24/05/2019	Include Polarization (chapter 4)
	24/05/2019	Include Uncertainty estimation procedure (chapter 5) : source notes Emma Woolliams
0.4	08/07/2019	All sections, added figures uncertainty
0.5	16/08/2019	Added uncertainty section, Added section on model output
0.6	09/09/2019	Updated sections except part 3
0.7	4/11/2019	updated section on uncertainty, showing new results with the updated measurements and derived models
0.8	18/11/2019	updated all sections
0.9	07/12/2019	Reviewed by Emma Woolliams
1	12/12/2019	Approved by Marc Bouvet
1.1	18/12/2019	update with new measurements : • New model coefficients • Measurements geometry overview • Update uncertainty analysis
1.2	03/12/2020	update with new measurements : • New model coefficients • Measurements geometry overview • Update uncertainty analysis
1.3	31/02/2022	update with new measurements : • New model coefficients • Measurements geometry overview • Update uncertainty analysis • Update DOLP model (2.7) • Fig 3,4,5,7,8,17 updated

1.1.1.1.4 Contents

1 Introduction

1.2 Purpose and Scope

This document describes the algorithmic and theoretic basis of the lunar irradiance model. It includes the method to adjust the model parameters based on irradiance measurements. It also describes how to propagate the uncertainties throughout the entire model chain.

1.3 Applicable and reference documents

1.3.1 Applicable Documents

The following applicable documents are those specification, standards, criteria, etc. used to define the requirements of this representative task order.

Number	Reference
[AD1]	ESA-TECEEP-SOW-002720. Lunar spectral irradiance measurement and modelling for absolute calibration of EO optical sensors.
[AD2]	Deliverable-1
[AD3]	Deliverable-2
[AD4]	Deliverable-3
[AD5]	Deliverable-4
[AD6]	Deliverable-6

1.3.2 Reference Documents

Reference documents are those documents included for information purposes; they provide insight into the operation, characteristics, and interfaces, as well as relevant background information.

Number	Reference
[RD1]	H.H. Kieffer and T.C. Stone. The Spectral Irradiance of the Moon. 2005. The American Astronomical Society. DOI:10.1086/430185.
[RD2]	Apollo 16 Samples from http://www.planetary.brown.edu/
[RD3]	Numerical Recipes in C, William H. Press . . . [et al.]. – 2nd ed.

[RD4]	SPICE : https://naif.jpl.nasa.gov/naif/documentation.html
[RD5]	Optical measurements of the Moon as a tool to study its surface, Y. Shkuratov et all, 2011
[RD6]	MODIS and SeaWIFS On-Orbit Lunar Calibration, Sun J. et All, 2008
[RD7]	On-orbit Radiometric Calibration Over Time and Between Spacecraft Using the Moon, Kieffer H. et all, 2003
[RD8]	Lunar Calibration Of MSG/SEVIRI Solar Channels, Viticchie et all, 2014

1.4 Glossary

1.4.1 Abbreviations

Abbreviation	Stands For	Notes
ESA	European Space Agency	Project customer
NPL	National Physical Laboratory	Project partner
J2000	Celestial reference frame for coordinates	
JPL	Jet Propulsion Laboratory	
NAIF	Navigation and Ancillary Information Facility	
ROLO	Robotic Lunar Observatory	
SPICE	Spacecraft Planet Instrument C-matrix Events	
SWIR	Short-Wave InfraRed	
USGS	U. S. Geological Survey	
UVa	University of Valladolid	Project partner
VITO	Flemish Institute for Technological Research *(Vlaamse Instelling voor Technologisch Onderzoek)*	Project partner
VNIR	Visual and Near InfraRed	

2 Lunar irradiance model derivation

2.1 Rationale

The moon has already been observed for thousands of years. These observations have, in recent years, evolved into detailed and automated radiometric measurements. Different measurements from various locations are being carried out: ground-based sensors, satellite sensors and even lunar orbiting sensors.

With the Robotic Lunar Observatory (ROLO), USGS has acquired 85000+ images of the moon, during a period of almost 10 years [KIEFER and STONE,2005]. The moon-disk-integrated irradiance was measured in 32 bands of which 23 are VNIR and 9 SWIR. About 1000 images per spectral band were used to fit the lunar spectral reflectance ROLO model. This reflectance model can be used to simulate any lunar irradiance up to 90 degrees phase angle. Many inter-comparisons between the ROLO model and e.g. space-born sensors have revealed a possible discrepancy in absolute levels of the model ([RD6][RD7][RD8]). These studies have shown a possible underestimation of the ROLO model by 5 % to 15 % in the VNIR and SWIR with respect to the satellite-based lunar observations. Some studies also indicate that there is a model dependency on the phase angle [RD8].

In this project, a new lunar irradiance model has been developed, based upon lunar measurements acquired with the CE318-TP9 instrument (also referred to as the 1088 instrument) . The development of the new model is based on the analytical formulation of the ROLO model with new estimates of the calibration parameters. However, where needed, the formulation was adapted.
At the UVa institute in Izaña (Tenerife), a second CIMEL instrument has been used to measure the lunar irradiance (also referred to as 933). This instrument was deployed during the period 2016 and 2017. New measurements with the 933 instrument have been conducted in the period 2018 and 2019, ensuring overlap between the two instruments.

The measurements of this instrument are used in this study to investigate the feasibility of the derivation of a new lunar irradiance model. The final model however will consist of 1088 results only, once sufficient measurements have been acquired. At the time of writing, measurements with the 1088 instrument are available for 2 years, from 03/2018 until 06/2018. About 160 irradiance measurements have been recorded. Added to that the 933 measurements, about 550 measurements per spectral in total are used in this study.

2.2 Lunar model definition

The model is based on the lunar irradiance measurements from the CE318-TP9 “1088” instrument (see D2, D3, D4 and D6 from this study)

The model is detailed in equation 1. It is a slightly modified version of the USGS ROLO lunar model [RD1].

The only difference is that for each spectral band in the model an independent set of *c*-coefficients has been defined, while in the original model, the *c*-coefficients are identical for all bands.

$$\ln(A_k) = \sum_{i=0}^{3} a_{ik} g^i + \sum_{i=1}^{3} b_{ik} \Phi^{2i-1} + c_{1k}\theta + c_{2k}\phi + c_{3k}\Phi\theta + c_{4k}\Phi\phi + d_{1k} e^{-\frac{gC}{p_1}} + d_{2k} e^{-\frac{gC}{p_2}} + d_{3k}\, cos\left(\frac{gC - p_3}{p_4}\right) \quad (1)$$

k is model spectral band,

A is the lunar reflectance, ln(*A*) the natural logarithm of *A*,

g is the absolute phase angle [radians],

θ selenographic latitude observer [degrees],

ϕ selenographic longitude of the observer [degrees],

Φ selenographic longitude of the Sun [radians],

$C = \frac{180}{\pi}$ conversion radians to degrees.

The reflectance model can be split-up in four different sections.

The **basic photometric function** is represented by the first polynomial depending solely on the phase angle. It is a wavelength-dependent third degree polynomial, described with the a_k^i coefficients.

The variations of the reflectance of the moon due to changes in the actual area **of the Moon illuminated by the sun** and driven by changes in the distribution of maria and highlands, is expressed in the second polynomial. This polynomial is depending only on the solar selenographic longitude Φ. Fourth order coefficients b_{ik} are defined for every wavelength.

The third section, with four wavelength dependent coefficients c_{ik}, represents the **visible part of the Moon** and how it is illuminated (topographic libration).

The last part of the equation is a set of parameterized exponential and cosine functions modulated by a set of d_{ik} coefficient: it is an **empirical iterative least squares fitting** of **non-linear residuals** in the irradiance, with respect to the phase angle.

The output reflectance of the model, with varying phase angle is shown in Figure 1.

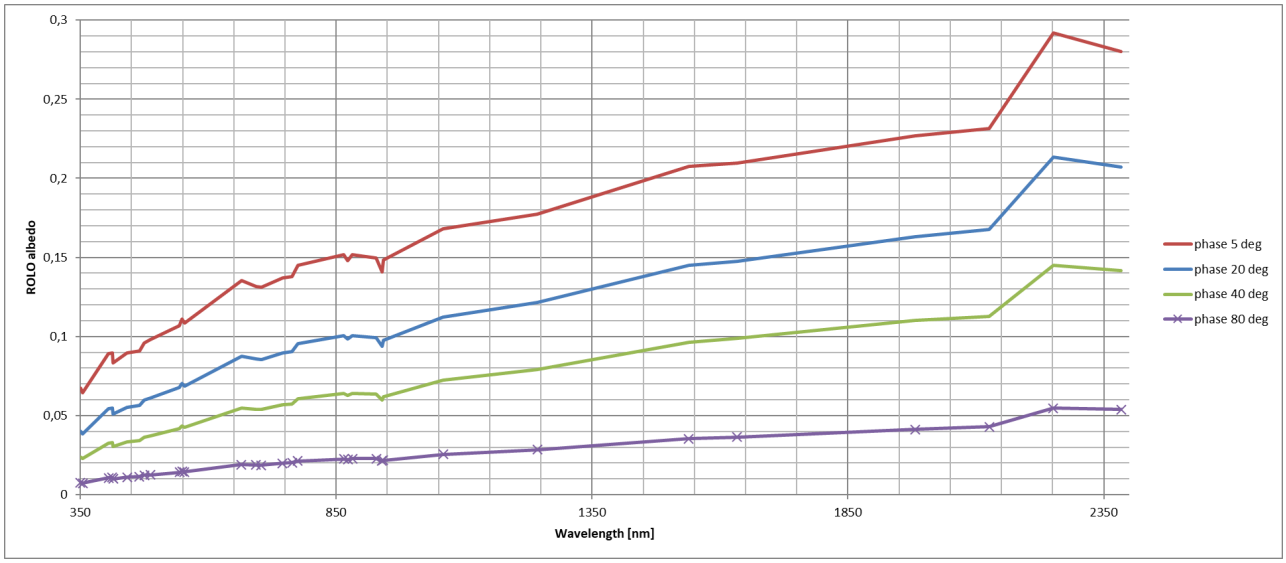

Figure 1: ROLO model reflectance spectrum output for different phase angles.

2.3 Geometric Calculations

2.3.1 Definition

Although the geometric calculations for Moon, Sun and observer are not explicitly part of the model, it is useful to mention that they are done using the JPL NAIF spice library. The software is available from: https://naif.jpl.nasa.gov/naif/

From the observation timestamp and exact topographic position it is possible to calculate in the J2000 celestial frame the position of observer, sun and moon.

With these positions, all inputs for the lunar reflectance model are defined: g, θ, ϕ, Φ.

The JPL NAIF spice library provides a set of kernels to define the position and motion vectors of the different celestial bodies involved in the geometric calculation:

List of kernels used to configure the spice library :

Kernel name	**Kernel type**
`naif0010.tls`	Leap-seconds (for UTC)
`pck00010.tpc`	Planetary constants
`earth_000101_130520_130227.bpc`	Planetary constants - earth
`earth_070425_370426_predict.bpc`	Planetary constants - earth
`moon_pa_de421_1900-2050.bpc`	Planetary constants - moon
`de421.bsp`	Ephemeris - earth
`earth_assoc_itrf93.tf`	Reference frame ITRF93
`moon_080317.tf`	Reference frame Moon
`moon_assoc_me.tf`	

Table 1: SPICE kernel list used in geometric calculations

2.3.2 Geometric coverage

There are many periodic cycles that apply to the Moon, Earth and Sun geometry. The cycle with the longest period is called the Saros cycle and its duration is 223 synodic months, which is 18 years, 11 days and 8 hours. After this cycle, Earth, Moon and Sun return to the same relative geometry.

The shortest cycle is the variation in phase angle which takes about 28 days between two full moons. The cycle for the distance between Sun and Earth/Moon takes about one year..

The complete Saros cycle covers all possible relative positions between Moon, Earth and Sun. Ideally, measurements need to be done for the entire cycle to get a complete coverage of the libration between all three bodies. This is not feasible within the scope of a project like this. Fortunately, about 6 years of daily measurements from an Earth fixed position are sufficient to homogeneously sample the space of possible selenographic latitude/longitude and phase angles occurring during the lunar cycle. In Figure 2 the corresponding selenographic latitude and longitude and phase angles are displayed for a period of six years (simulated with SPICE [RD 2]). Phase angles above 90 degrees absolute are discarded. The regression of the model interpolates between the measured librations.

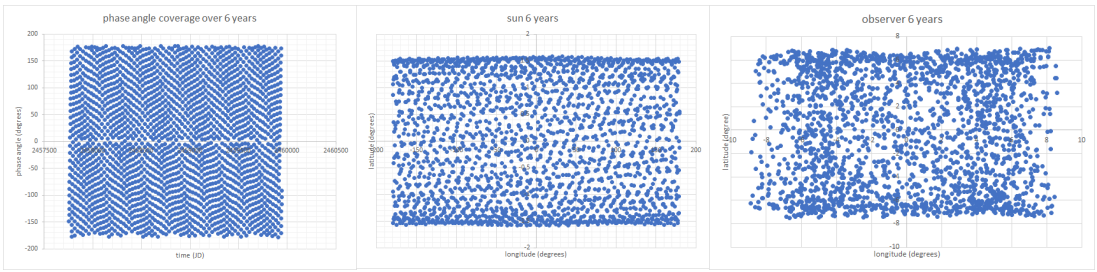

Figure 2: Phase angle, solar and observer selenographic longitude and latitude coverage for 6 years continuous observations

Plots of geometry of the measurements show the limited coverage, compared to the previous plot. However, the most recent plots including all 1088 instrument measurements (3.5 years of measurements), currently reveal a significantly increased libration coverage.

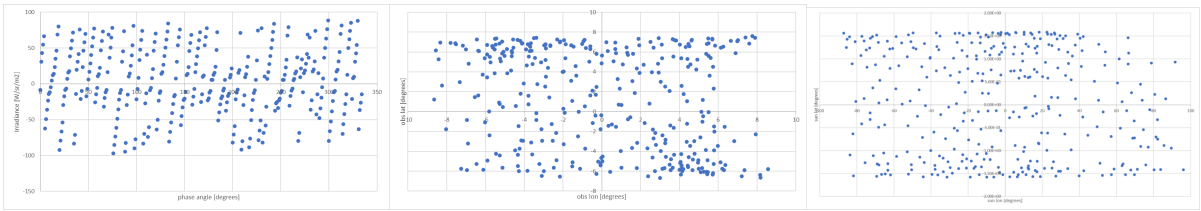

Figure 3: Phase angle, solar and observer selenographic longitude and latitude coverage for the 1088 instrument after 3.5 years of measurements

2.4 Lunar Measurements

Figure 4 is a plot of approximately three years' lunar irradiance measurements with the 440 nm spectral band relative to the phase angle. Both 933 and 1088 instrument measurements are plotted. The irradiance is normalized for distances between sun, moon and observer at the time of observation.

The irradiance is converted to reflectance values using the following formula. All further model derivation is performed on the disc equivalent reflectance.

$$A_\lambda = \frac{I_\lambda \pi}{\Omega_M E_\lambda} \tag{2}$$

A_λ lunar reflectance for a wavelength λ

I_λ measured irradiance

E_λ extra-atmospheric solar irradiance

Ω_M solid angle of the Moon (6.4177×10^{-5} sr)

The solar irradiance spectrum used is the Werhli 1985. It is the same as the one used with the development of the ROLO model, which allows for comparison of the model reflectance output. Replacement with other irradiance standards is possible, but the same model needs to be applied when converting back from reflectance to irradiance (i.e. when comparing with other Lunar irradiances).

Figure 4 is the plot of all irradiance measurements used in the derivation of the model (instrument 440 nm band). 3-sigma filtering is applied to the original measurements.

Close to full moon there is an apparent increase in scattering in the lower phase angles. However, in Figure 5, after removal of outliers, the relative residuals between the measurements and the model appear to be independent of the phase angle.

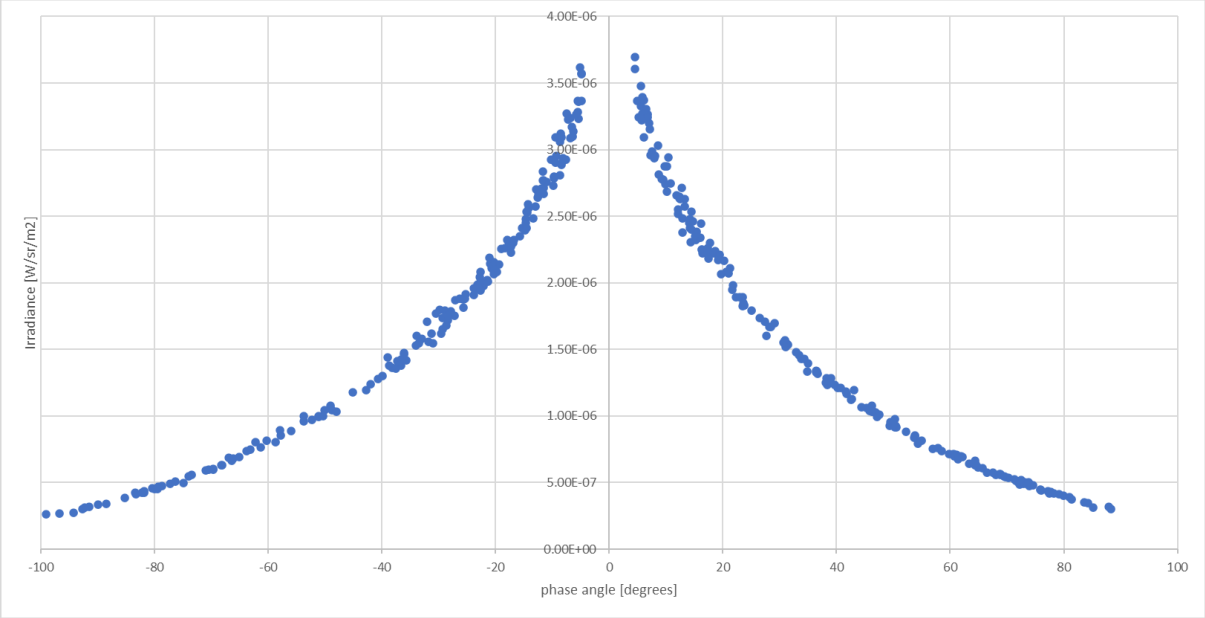

Figure 4: Lunar irradiance measurements for 440 nm

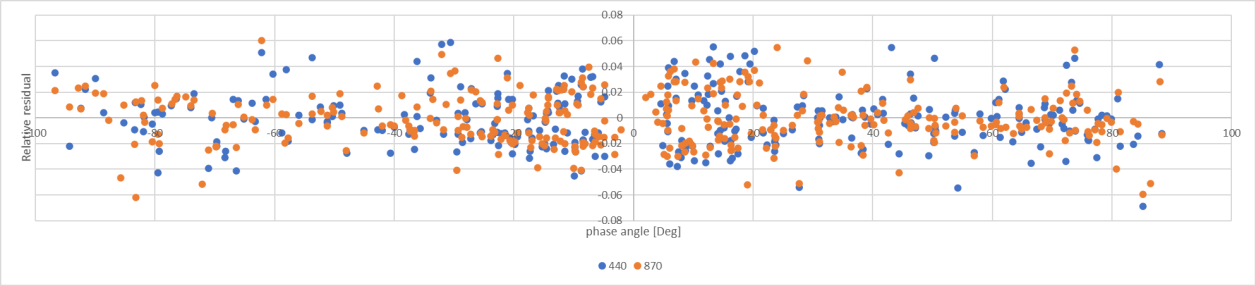

Figure 5: Relative residuals between measurements and model for 440nm and 870nm

2.5 Lunar irradiance model coefficient regression

The equation 1 models the natural logarithm variations of the disc equivalent reflectance. The parameters a_{ik}, $b_{ik,}$ c_{ik} and d_{ik}can be derived from direct irradiance measurements with the 1088 instrument, for all spectral bands.

The model equation can be split in two main components, representing a linear part and a non-linear part. The regression strategy is also separate for each part. There is also a distinction between band specific coefficients and the ones that are fitted for all six spectral bands.

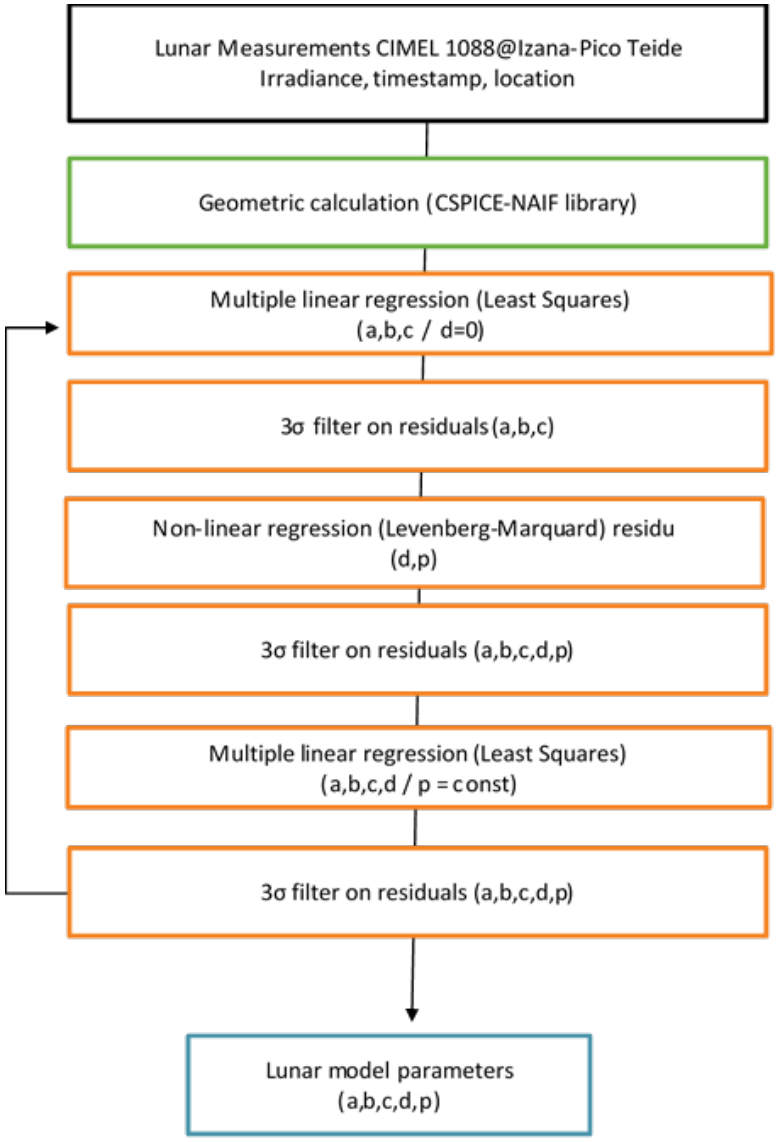

Figure 6: Lunar model coefficients regression algorithm

First, a least-squares fit on the linear part of the model is calculated, by putting all *d*-parameters in equation 1 to zero. First, the *a*, *b* and *c* band specific coefficients are derived. With this set of coefficients, (*a*, *b* and *c*), a first 3 sigma outlier removal is done.

Then, a regression is performed on the non-linear part of the equation, using the Levenberg-Marquardt method. The *d* and *p* parameters are calculated using the residuals of all bands (Figure 8). The *p* parameters are then used in further regression and outlier removals.

Finally, again a full linear fitting is performed on the entire equation, keeping the previously derived non-linear parameters constant (*p*-parameters).

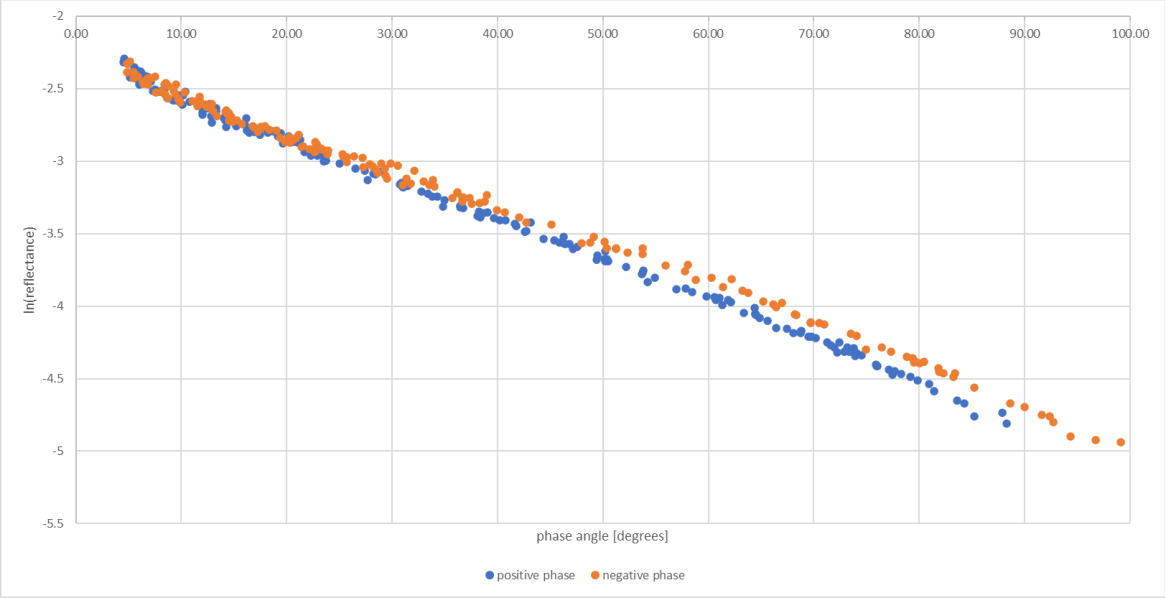

Figure 7: Natural logarithm of lunar reflectance measurement against absolute phase angle [degrees]. Negative and positive angles plotted separately

2.5.1 Linear model fitting procedure

The first step in the regression approach is regression on the linear part of the model : in Figure 7, the natural logarithm of the measured reflectance is taken before doing the first regression.

Multivariate linear regression is performed for the first three sets of coefficients, using the matrix approach. The linear part of the model is described by the first part of the model formula :

$$\ln(A_k) = \sum_{i=0}^{3} a_{ik} g^i + \sum_{i=1}^{3} b_{ik} \Phi^{2i-1} + c_{1k}\theta + c_{2k}\phi + c_{3k}\Phi\theta + c_{4k}\Phi\phi \tag{3}$$

The regression is calculated per band : one set of *a*, *b* and *c* coefficients, a total of 11 parameters, is determined simultaneously for each band using the following formulation :

$$\begin{pmatrix} y_1 \\ y_2 \\ \dots \\ y_n \end{pmatrix} = \begin{pmatrix} 1 & x_{11} & x_{12} & \dots & x_{1p} \\ 1 & x_{21} & x_{22} & \dots & x_{2p} \\ 1 & \vdots & \vdots & \ddots & \vdots \\ 1 & x_{n1} & x_{n2} & \dots & x_{np} \end{pmatrix} \begin{pmatrix} h_1 \\ h_2 \\ \dots \\ h_p \end{pmatrix}$$

The *X* matrix dimension in this formula is *n* * *p* :

- *n* number of measurements
- *p* number of coefficients to be fitted.

Definition of the parameters in the matrices :

- y_n the natural logarithm disc reflectance $ln(A_i)$
- x_{np} predicted p , calculated for measurement n
- h_p coefficient p

The *y* values are the natural logarithm for every measured reflectance *A*, the *x* values are all calculated predictor values. They are calculated using phase angle, solar selenographic longitude, observer selenographic longitude and latitude. Practically, the matrix is constructed with every factor the of the lunar model calculated, as if all *a*, *b* and *c* parameters are equal to 1.0 (see also X-matrix below).

The *h*-matrix represents the coefficients to be fitted and *e* the resulting fitting error. Rewriting the regression formula gives following matrix equation :

$$\mathbf{Y} = \mathbf{Xh} \tag{4}$$

After converting the formula, the solution for matrix ***h*** can be found (***X***′ is the transposed ***X*** matrix. $\boldsymbol{X}^{-1}$ is the inverse of ***X***.

$$\mathbf{h} = (\mathbf{X}'\mathbf{X})^{-1}\mathbf{X}'\mathbf{Y} \tag{5}$$

Steps to calculate the resulting ***h*** matrix :

> First you calculate ***X***′, then you multiply ***X***′ and ***X***, which results in a squared matrix of dimension $n \times n$. The inverse of this new matrix ***A*** is calculated using LU decomposition using Crout's algorithm with partial pivoting.

Construction of the matrix ***X*** is done by filling in the predictors at their matrix position, for every measurement. For band *k* and *n* measurements, the construction of the matrix is as follows :

Definition of the *X* matrix is as follows :

$$\begin{matrix}
1 & g^1_{1k} & g^2_{1k} & g^3_{1k} & \Phi^1_{1k} & \Phi^3_{1k} & \Phi^5_{1k} & \theta_{1k} & \phi_{1k} & \Phi\theta_{1k} & \Phi\phi_{1k} \\
\cdots & \cdots & \cdots & \cdots & \cdots & \cdots & \cdots & \cdots & \cdots & \cdots & \cdots \\
1 & g^1_{mk} & g^2_{mk} & g^3_{mk} & \Phi^1_{mk} & \Phi^3_{mk} & \Phi^5_{mk} & \theta_{mk} & \phi_{mk} & \Phi\theta_{mk} & \Phi\phi_{mk} \\
1 & g^1_{(m+1)k} & g^2_{(m+1)k} & g^2_{(m+1)k} & \Phi^1_{(m+1)k} & \Phi^3_{(m+1)k} & \Phi^5_{(m+1)k} & \theta_{(m+1)k} & \phi_{(m+1)k} & \Phi\theta_{(m+1)k} & \Phi\phi_{(m+1)k} \\
\cdots & \cdots & \cdots & \cdots & \cdots & \cdots & \cdots & \cdots & \cdots & \cdots & \cdots \\
1 & g^1_{nk} & g^2_{nk} & g^3_{nk} & \Phi^1_{nk} & \Phi^3_{nk} & \Phi^5_{nk} & \theta_{nk} & \theta_{nk} & \theta_{nk} & \Phi\phi_{nk}
\end{matrix}$$

The result is a $n \times 11$ matrix, for *n* measurements and 11 coefficients

Similarly, for the construction of the ***Y*** matrix, each irradiance measurement is first converted to reflectance *A* and the natural logarithm resulting in the *n* × 1 matrix:

$$\begin{matrix} \ln(A_1)_k \\ \cdots \\ \ln(A_m)_k \\ \ln(A_{m+1})_k \\ \cdots \\ \ln(A_n)_k \end{matrix}$$

After obtaining the coefficients, the remaining residuals represent the nonlinear part of the model. The procedure for retrieving the *d* and *p* coefficients is described in the next section. **After the nonlinear regression**, the linear regression procedure is repeated, using the selected measurements. The ***X*** matrix is expanded with factors for the *d* coefficients. All 14 linear coefficients are then fitted again for the remainder of the measurements.

$$\begin{matrix} e^{-\frac{g}{p_1}_k} & e^{-\frac{g}{p_2}_k} & cos\left(\frac{g-p_3}{p_4}\right)_k \\ \cdots & \cdots & \cdots \\ e^{-\frac{g}{p_1}_{nk}} & e^{-\frac{g}{p_2}_{nk}} & cos\left(\frac{g-p_3}{p_4}\right)_{nk} \end{matrix}$$

2.5.2 Non - Linear fitting procedure

These residuals (Figure 8) will be used to fit the non-linear part of the model. To obtain the band independent parameters (p), regression will be done based on the Levenberg-Marquardt [RD3] method.

$$Res = d_{1k}e^{-\frac{g}{p_1}} + d_{2k}e^{-\frac{g}{p_2}} + d_{3k}\cos\left(\frac{g-p_3}{p_4}\right) \quad (2)$$

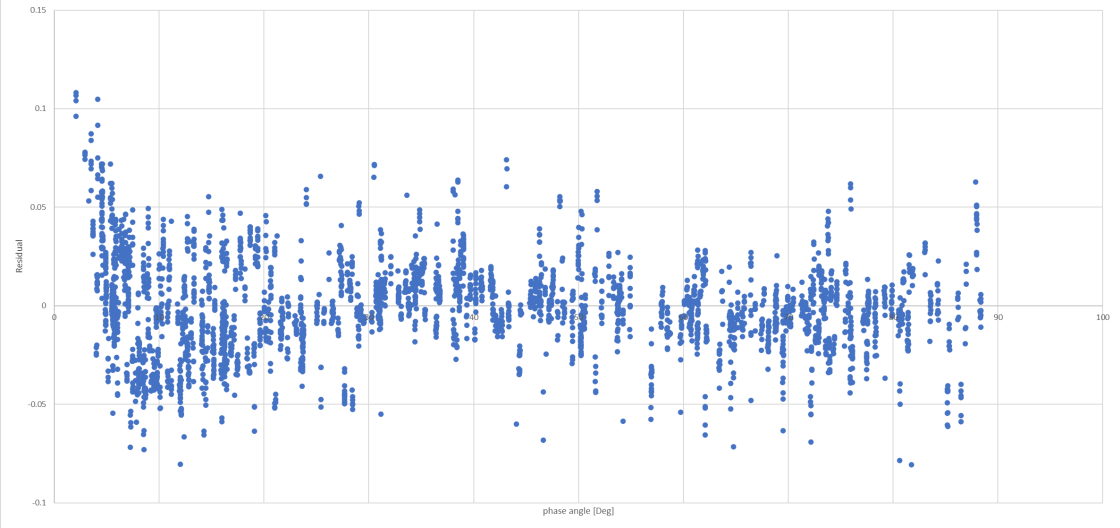

Figure 8: Model residue (in the fitted parameter ln*(A)) after linear fitting process for all bands*

The non-linear part of the lunar reflectance model depends on the measurement phase angle. From the residuals calculated with previous steps, the next non-linear relationship is fitted. For convenience all 7 fitting parameters *d* and *p*. In the first iteration, all *a* parameters will be fitted against all bands. In the second iteration the *p*-parameters are adopted from the first fitting. From that point, the *d* parameters are re-fitted, but band specific and in a linear least squares fitting with all *a*, *b* and *c* parameters.

Based on the calculation of the merit-function. The model has to be fitted :

Model :

$$y = y(x; a) \qquad (3)$$

Merit-function :

$$\chi^2(\mathbf{a}) = \sum_{i=1}^{N} \left[\frac{y_i - y(x_i; \mathbf{a})}{\sigma_i} \right]^2$$

For every $\mathbf{a_k}$ one can calculate the derivative of the merit function : $k = 1 \ldots M$ with M the number of parameters (7 in our case).

$$\frac{\partial \mathcal{X}^2}{\partial a_k} = -2\sum_{i=1}^{N}\left[\frac{y_i - y(x_i;\,\mathbf{a})}{{\sigma_i}^2}\right]\frac{\partial y(x_i;\,\mathbf{a})}{\partial a_k}$$

And additional partial derivatives :

$$\frac{\partial^2 \partial \mathcal{X}^2}{\partial a_k \partial a_l} = 2\sum_{i=1}^{n}\frac{1}{{\sigma_i}^2}\left[\frac{\partial y(x_i;\,\mathbf{a})}{\partial a_k}\frac{\partial y(x_i;\,\mathbf{a})}{\partial a_l} - \left[y_i - y(x_i;\,\mathbf{a})\right]\frac{\partial^2 y(x_i;\,\mathbf{a})}{\partial a_l \partial a_k}\right]$$

This can be rewritten as a set of linear equations :

$$\sum_{l=1}^{M}\alpha_{kl}\delta a_l = \beta_k$$

With

$$\beta_k \equiv -\frac{1}{2}\frac{\partial \mathcal{X}^2}{\partial a_k}$$

and

$$\alpha_{kl} \equiv \frac{1}{2}\frac{\partial^2 \partial \mathcal{X}^2}{\partial a_k \partial a_l}$$

2.5.3 Residual outlier removal approach

After removing all measurements outside the filter interval [-90;90] degrees, a filter approach as applied to the residuals of the measurements. The residuals are calculated based on the model parameters that have been derived at

3 sigma filter procedure:

res_i residuals for i^{th} measurement

N total numer of measurements (i)

$$res_{mean} = \frac{\sum res_i}{N}$$

$$s(res) = \sqrt{\frac{1}{N}\sum_{i=1}^{N}(res_i - res_{\text{mean}})^2}$$

res_{mean} is the mean residual and *s(res)* is the residuals standard deviation. A 3-sigma filter (99.7% confidence interval) is applied, to remove outlier measurements. This filter is applied multiple times during the coefficient regression procedure.

$$res_{\text{mean}} - 3s(res) < res_i < res_{\text{mean}} + 3s(res)$$

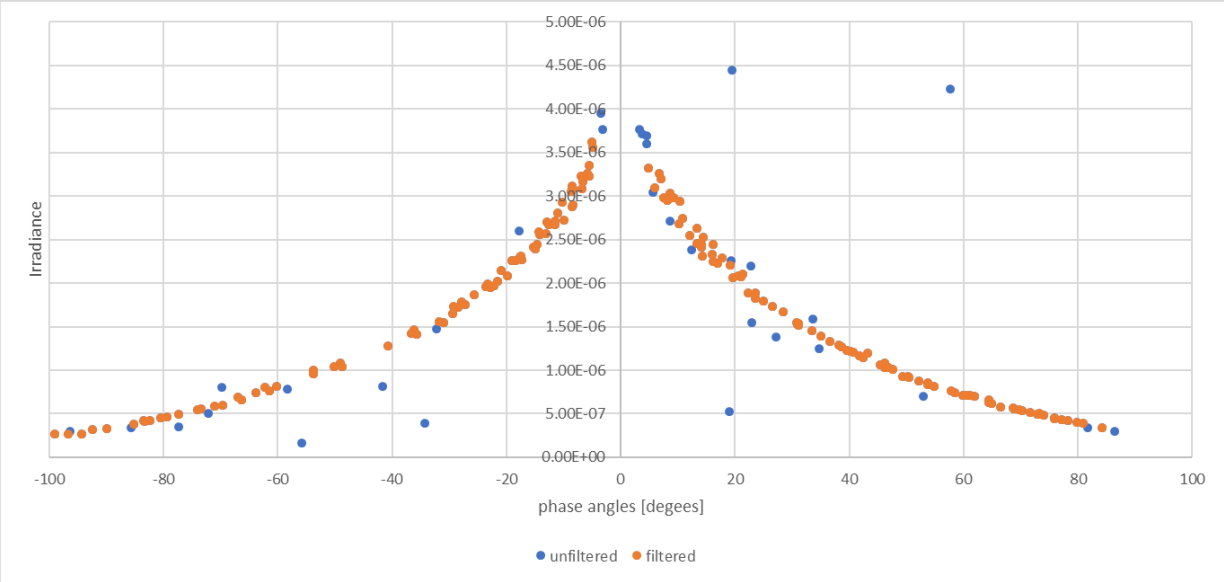

Figure 9: Filtered vs unfiltered irradiance (restricted number of measurements for illustration)

As an example, one can see the filtering result in Figure 9. Blue dots are filtered out after applying the 3 sigma filter to the residuals.

2.5.4 Iterative regression procedure

Outliers influence the results of the regressions quite significantly, so they need to be removed from the measurement population as much as possible. After all regression steps, the 3-sigma filter is applied.

Regression sequence :

- Fit the linear coefficients *a*, *b* and *c* (all *d* coeffs equal to zero)
- Remove outlier 3-sigma from the residuals :
    - Residual = (measurement irradiance – model as is)
- Perform non-linear regression for d-coefficients and p-coefficients
- Remove outlier 3-sigma from the residuals
- Perform fitting over all linear coefficients : a,b,c,d (non-linear coefficients previous step)
- Remove outliers based on residuals full model

After the first iteration, a second full iteration is performed

2.5.5 Model coefficients 1088 instrument

Within the period 03/2018 until 12/2021,about 400 lunar irradiance measurements have been performed (depend per spectral band) and after filtering the data, based upon the quality of the Langley plots, between 230 and 260 retrievals have been used to derive the model parameters in Table 2.

wl[nm]	**a0**	**a1**	**a2**	**a3**	**b1**	**b2**	**b3**
440	-2.26317	-1.95341	0.691585	-0.30189	0.052456	0.008714	-0.00415
500	-2.15048	-1.82816	0.59675	-0.27933	0.050078	0.010695	-0.00382
675	-1.91452	-1.72298	0.562315	-0.2762	0.047094	0.012212	-0.00484
870	-1.81647	-1.5906	0.465803	-0.24815	0.046823	0.018782	-0.007
1020	-1.75279	-1.50502	0.401689	-0.22989	0.052412	0.021768	-0.00864
1640	-1.47438	-1.21778	0.189073	-0.16837	0.047555	0.011999	-0.00487
wl[nm]	**c1**	**c2**	**c3**	**c4**	**d1**	**d2**	**d3**
440	0.001217	-0.00036	0.00161	0.000732	-0.09294	2.000626	-0.00571
500	0.001117	-0.00041	0.00178	0.000945	12.96653	-12.422	-0.00273
675	0.001113	-0.00043	0.00171	0.000936	9.886489	-9.75239	-0.00594
870	0.001153	-3.74E-04	0.001882	0.000895	10.47813	-10.3637	-0.00342
1020	0.001044	-4.50E-04	0.001817	0.000837	11.93628	-11.8154	-0.00255
1640	0.000945	-4.90E-04	0.001732	0.001093	14.32673	-14.4102	3.48E-06
	p1	**p2**	**p3**	**p4**			
all	1.35446	1.314674	9.324089	9.596769			

Table 2: Model coefficients

With these model coefficients, the lunar reflectance is calculated for every model wavelength.

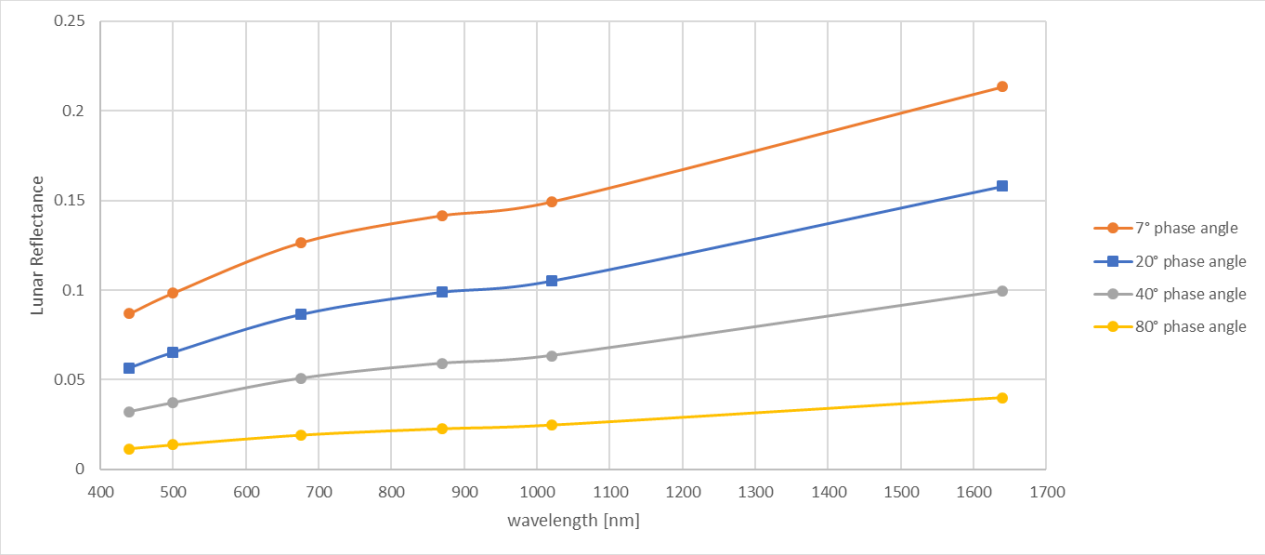

Figure 10: Lunar reflectance per wavelength for different phase angles. Interpolated values only for visual guidance, not the actual spectral interpolation

It must be noted that these coefficients are currently under development and not final. The model will be updated on a yearly basis, based upon new measurements added to the measurement database.

2.6 Lunar irradiance model output

With the model parameters tabulated in Table 2, the lunar reflectance can be calculated for the model spectral bands (Figure 10). The model output wavelengths correspond to the lunar photometer spectral bands. The reflectance values obtained from the model are subsequently used as absolute references to radiometrically scale a hyperspectral lunar reflectance spectrum. This radiometrically rescaled hyperspectral lunar reflectance spectrum can be convolved with at a given remote sensing instrument spectral response curves and simulated remote sensing instrument observations. The model inputs are lunar phase angle, selenographic positions of sun and observer and a band response curve to which the model irradiance needs to be convolved.

2.6.1 Spectral model adjustment

A reflectance spectrum of the Moon is used to increase the model spectral resolution. The lunar model calculates the reflectance at 6 wavelengths. The spectral range of the model goes from 440 nm to 1640 nm. Therefore, in intermediate model regions, the spectrum needs to be adjusted and reconstructed.

First step is the smoothing of the measured spectrum with a reference reflectance. The lunar model allows for a flexible configuration of the reflectance spectrum. In the current configuration, the original Apollo spectrum can be used, or the spectrum derived from measurements with the Pandora instrument. The Pandora instrument measurement campaign has been conducted over a full lunar phase cycle. This allows for the adjustment of the reflectance model based on the phase angle. This will be done by linear interpolation. The reflectance spectra shown in Figure 11 show a difference between the Pandora and the Apollo spectrum. The Pandora spectrum is taken for one specific day. It

is currently still under investigation why in many cases the measured Pandora reflectance deviates quite a lot in absolute terms, from the Apollo spectrum.

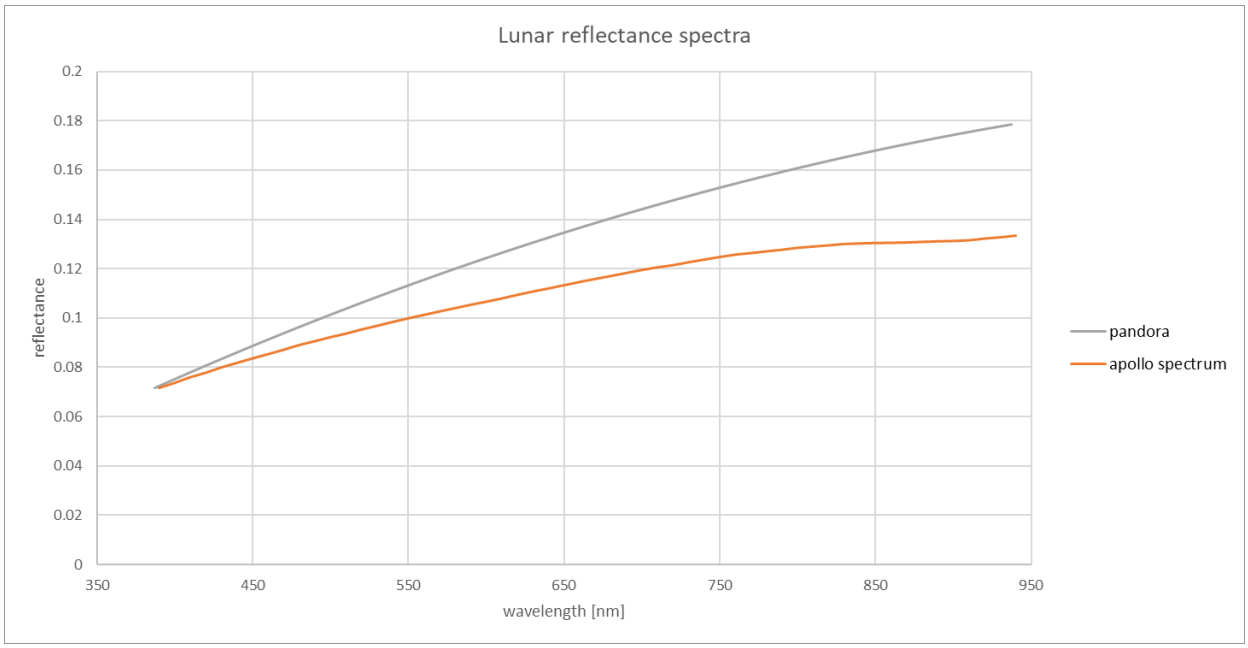

Figure 11: Difference Apollo and Pandora spectrum

In this study, the Apollo spectrum mix is used to calculate the lunar spectral irradiance. The lunar model is the absolute reflectance reference for the different wavelengths, the reflectance spectrum is the spectral reference.

For a given geometry (phase angle, libration, …) the lunar model provides a reflectance for all 6 model bands. Then, the reflectance spectrum is convolved with the model spectral band responses (i.e. the CE318-TP9 instrument), providing a second reflectance at every model spectral band. Both reflectances are used to define the smoothing parameters by means of Least Absolute Deviation (LAD) regression.

LAD regression general formulation :

$$y(x; a, b) = a + bx$$

Function to minimize (*N* is the number of model wavelengths):

$$\sum_{i=1}^{N} |y_i - a - bx|$$

The median minimizes the sum of absolute deviations and for a fixed *b*, the value of a that minimizes is :

$$a = \text{median}\{y_i - a - bx_i\}$$

Regression parameter *b* is found by bracketing and intersection of next function (a can be filled in) :

$$0 = \sum_{i=1}^{N} x_i sgn(y_i - a - x_i)$$

From the LAD regression parameters, the full reflectance spectrum is converted/adjusted. The smoothing adjustment is applied to the measured reflectance spectrum

$$R\_\text{smooth}_\lambda = bR_\lambda + a$$

As can be observed in Figure 1, the output of the ROLO model is subjected to irregular variations with respect to wavelength. Therefore, a procedure for smoothing of the reflectance is proposed in [RD1].

Reflectance profiles of two Apollo 16 lunar probe samples are used, to construct a reference reflectance spectrum. This spectrum is used to radiometrically rescale and interpolate the ROLO model output at the ROLO measurement spectral bands.

The resulting reflectance $R\text{mix}_\lambda$ is a linear combination of both spectral (λ) reflectance's.

$$R\text{mix}_\lambda = 0.05 \times R\text{breccia}_\lambda + 0.95 \times R\text{soil}_\lambda \ (4)$$

In Figure 12 you can observe the resulting mixed reflectance (in green) of the Apollo 16 breccia sample (red line) and Apollo 16 soil sample (dark blue line).

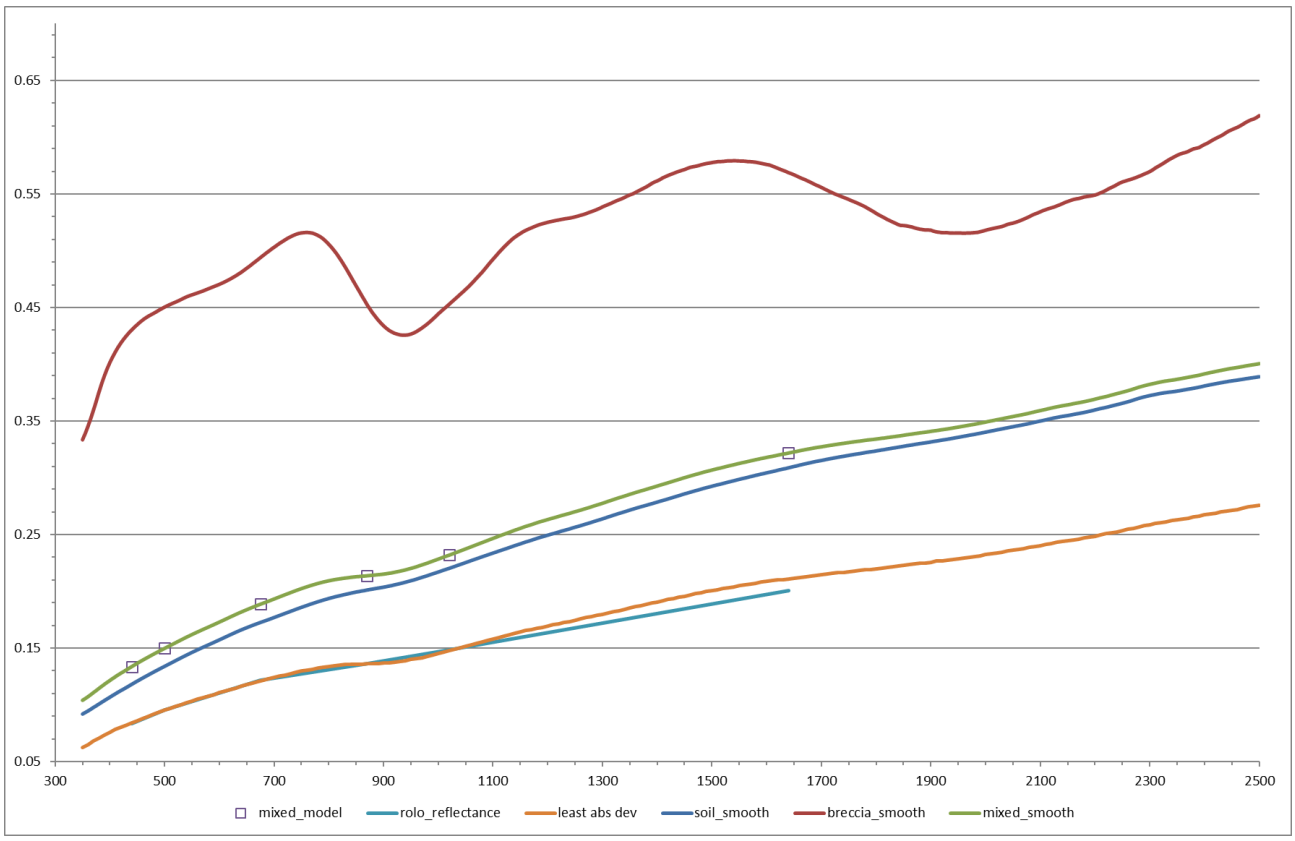

Figure 12: Lunar reflectance spectral smoothing

The mixed reflectance is derived for every lunar model wavelength of the model (purple dots on the green curve). These values are used to calculate the least absolute deviation regression values. The lunar model reflectance's used in the regression are calculated for every measurement specifically.

This regression results in a set of smoothing coefficients, which are applied to the spectral reflectance model, resulting in a smoothed lunar reflectance spectrum.

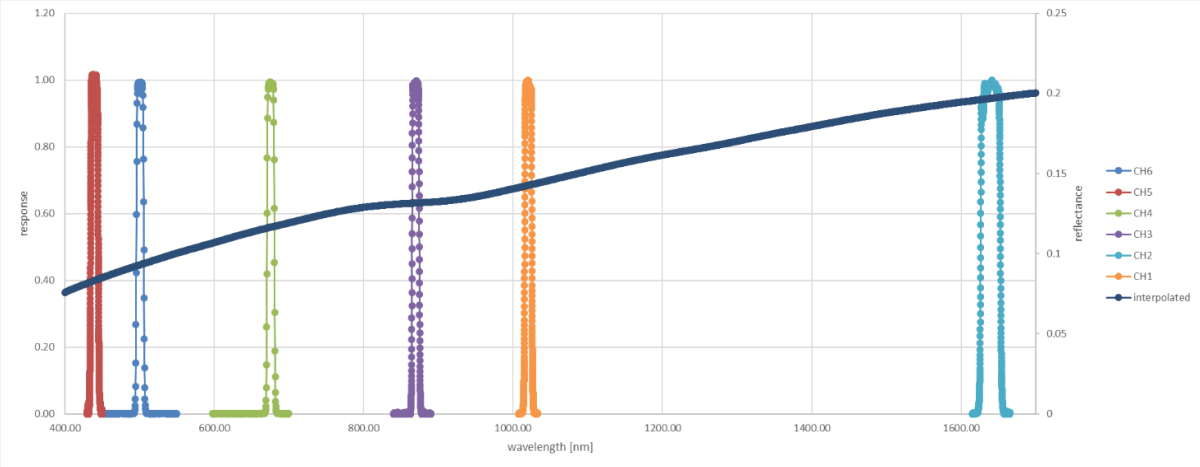

Figure 13: Cimel response curves and interpolated smoothed reflectance

The approach is applied both to the Apollo spectrum and the available Pandora reflectance spectrum. For the 440nm spectral band Figure 14 shows that the difference between final model irradiance and instrument measurement irradiance is quite similar for both spectral models. With the Apollo reflectance spectrum, a slightly increased phase angle dependency can be observed (orange dots). Further investigation is required when, in a next iteration of the model, the reflectance spectrum is extended up to 2500 nm with ASD measurements. The Pandora spectrum by itself only reaches up to 940 nm.

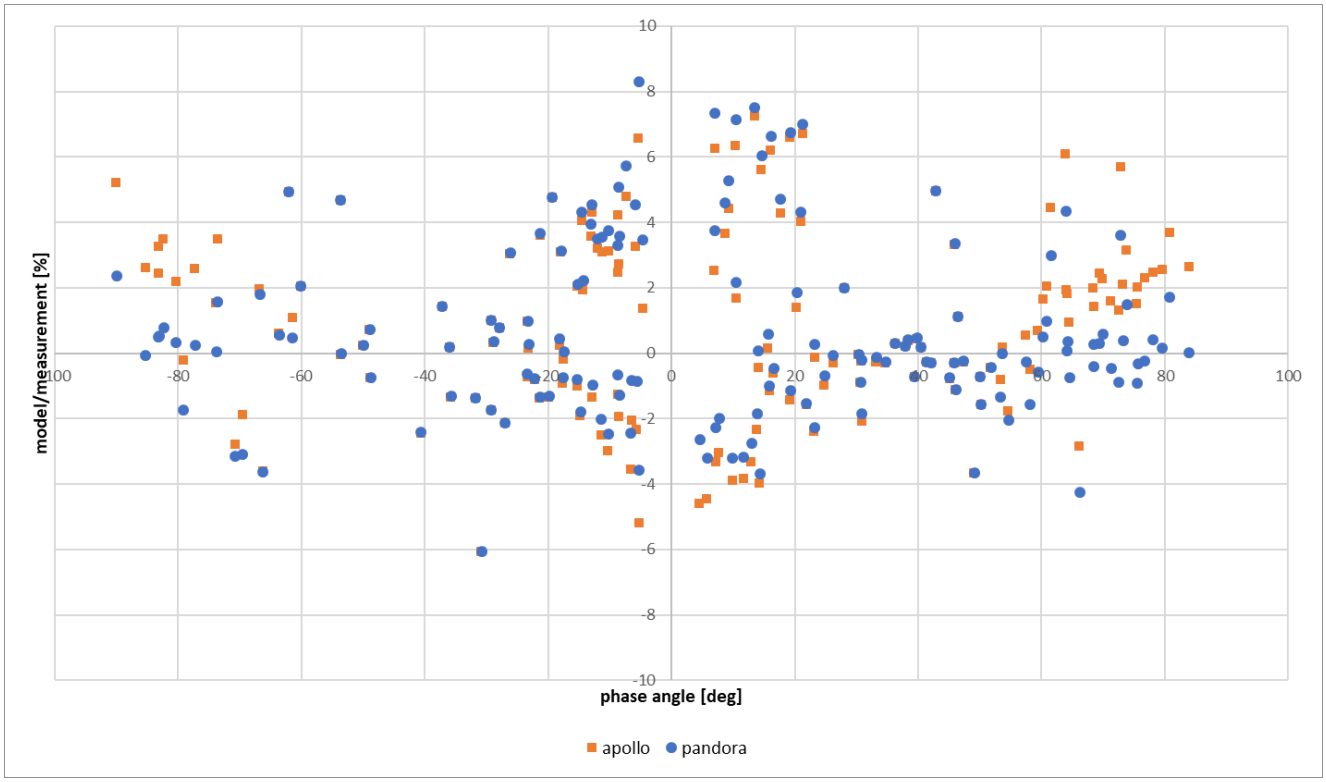

Figure 14: Residual between measurement and model for Apollo and Pandora reflectance spectrum (for illustration with previous measurement dataset)

2.6.2 Simulating lunar irradiance measurements from the lunar irradiance model

The reflectance spectrum obtained in the previous section is converted to irradiance, and then convolved with a given remote sensing instrument relative spectral response (e.g: a multi-spectral instrument). By means of cubic spline interpolation, the reflectance spectrum is resampled to the relative spectral response wavelengths and then convolved with the model simulated lunar irradiance spectrum.

First, the second derivative of the entire spectrum is calculated. The interpolation between 2 points (*j* and *j*+1) is defined by :

$$y = ay_j + by_{j+1} + cy_j'' + dy_{j+1}''$$

For every wavelength point of the response curve, interpolation is calculated. Then the integral normalized by the integral of the Relative Spectral Response (RSR) of the sensor is calculated.

$$I_k = \pi * \Omega_M * \frac{\sum_{i=\lambda_0}^{\lambda_n} Refl_i * E_i * RSR_i * \lambda_i}{\sum_{i=\lambda_0}^{\lambda_n} RSR_i * \lambda_i} \quad (5)$$

I_k integrated lunar model reflectance for spectral band k

Refl interpolated lunar reflectance spectrum at the sensor RSR wavelengths

RSR band spectral response

λ wavelengths at which the sensor RSR are defined

E_i Exo-atmospheric solar irradiance

Ω_M solid angle of the moon (6.4177×10^{-5} sr)

This model irradiance value is the input for comparison with lunar acquisitions done with the band represented by the RSR provided to the model.

2.7 Polarization

2.7.1 Introduction

The linear polarization of lunar reflected light has been studied and the phase angle dependency is described in [RD5]. Unusually, the lunar polarization shows negative linear polarisation at phase angles smaller than the inversion angle. This is the phase angle at which the polarisation becomes negative (22° absolute phase angle) [RD5].

The CE318-TP9 lunar photometer (1088 instrument) measures directly the degree of linear polarization of the moon. With these measurements, it is possible to derive a simplified model, based on linear regression. The model is defined per band and consists of 2 separate 4th degree polynomial functions, one for positive and one for negative phase angles.

2.7.2 Degree of linear polarization - measurements

The degree of linear polarization(DoLP) of a signal is defined as

$$P = \frac{\sqrt{Q^2 + U^2}}{I}$$

I, *Q* and *U* are the Stokes parameters that describe the polarization of electromagnetic radiation. The circular polarization component *V* is ignored.

The construction of the 1088 instrument prevents the Stokes parameters from being measured directly, but the DoLP can be calculated from the different instrument filter outputs. This implies however, that it is not possible to measure negative polarization. The way to convert the output of the instrument to Stokes parameters, or a way to calculate a negative solution of the DoLP formula, is currently under investigation.

For the purpose of this project, all measurements below the inversion angle are set to negative. This is a pragmatic approach the use the negative solution of the DoLP formula. This approach might be improved or refined in the future. This depends on the availability to derive Stokes parameters from measurements.

Three linear polarized filters are oriented 60° from each other, measuring directly the raw polarized signals. The three filters give a value for S_{p1} , S_{p2} , S_{p3}. The degree of polarization is derived with the following formula :

$$DoLP = \frac{2\eta\sqrt{S_{p1}^2 + R_{12}^2 S_{p2}^2 + R_{13}^2 S_{p3}^2 - R_{12}S_{p1}S_{p2} - R_{13}S_{p1}S_{p3} - R_{12}R_{13}S_{p2}S_{p3}}}{S_{p1} + R_{12}S_{p2} + R_{13}S_{p3}}$$

R_{12}, R_{13} are the corrections for total polarization transmittance and η is the polarization calibration coefficient. These are constant values, calculated during the calibration of the instrument.

All measurements performed in this project with the 1088 instrument are done with polarization enabled. This means for the period of about 1 year, more than 120000 measurements of lunar polarized light are available. Not all measurements are done at full night-time and these need to be filtered from the regression. The measurements are filtered on time – between 23h at night and 2h in the morning and outliers are removed (i.e. cloud contaminated measurement,…). Measurements with negative and positive phase angles are split to be able to produce a separate regression on both sides. About 25000 measurements per phase sign are used to perform the model regression. The spectral bands are treated separately.

2.7.3 Model

Publications have shown a negative polarization for phase angles smaller than 22 degrees (inversion angle)[RD5]. The method applied with the CE318-TP9 measurements do not allow for a negative phase angle. Therefore, it is currently decided, to allow for modelling to change the sign of all measurements between -22 and 22 degrees phase angle.

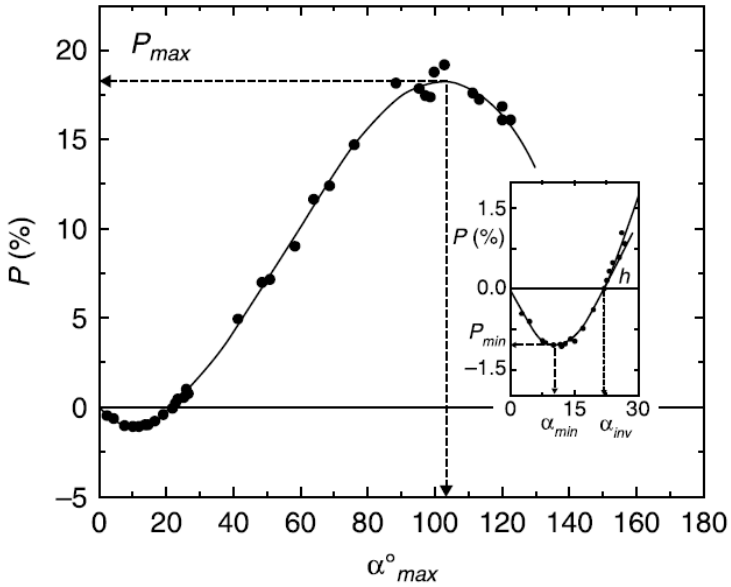

Figure 15: model for lunar DOLP curve with phase angle (Kvaratskhelia - 1988)

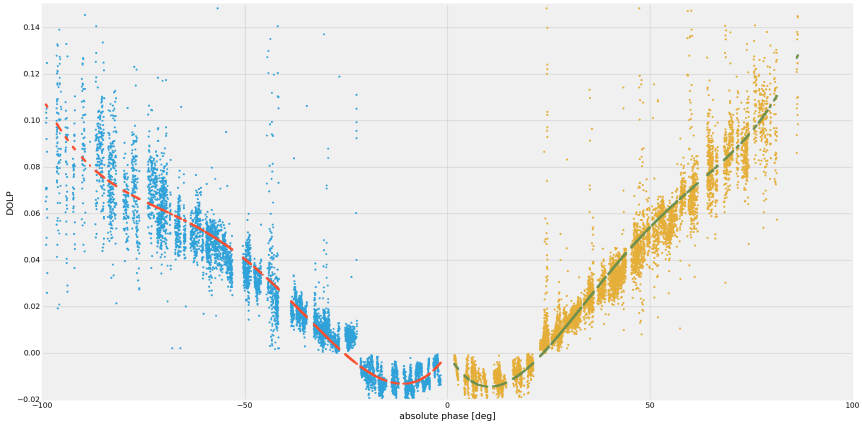

Figure 16: Curve fitted DOLP measurements for 500 nm *band*

The model is limited to be between 0° and 90° absolute phase angle. All polarization measurements outside these angles are removed from the regression of DoLP curves.

As can be observed in Figure 16, the DoLP can be modelled using a fourth order polynomial with the intercept set to zero. From this polynomial the DoLP value is calculated directly.

$$DOLP = a_1 \times g + a_2 \times g^2 + a_3 \times g^3 + a_4 \times g^4$$

g : is the phase angle in degrees

Table 3: Polynomial coefficients for DOLP

	negative				positive			
	a1	a2	a3	a4	a1	a2	a3	a4
440	0.003008799098	0.000177889155	0.000002581092	0.000000012553	-0.003328093061	0.000221328429	-0.000003441781	0.000000018163
500	0.002782607290	0.000161111675	0.000002331213	0.000000011175	-0.002881735316	0.000186855017	-0.000002860010	0.000000014778
675	0.002467126521	0.000140139814	0.000002021823	0.000000009468	-0.002659373268	0.000170314209	-0.000002652223	0.000000013710
870	0.002536989960	0.000150448307	0.000002233876	0.000000010661	-0.002521475080	0.000157719602	-0.000002452656	0.000000012597
1020	0.002481149030	0.000149814043	0.000002238987	0.000000010764	-0.002546369943	0.000158157867	-0.000002469036	0.000000012675
1640	0.002135380897	0.000126059235	0.000001888331	0.000000009098	-0.002726077195	0.000171190004	-0.000002850707	0.000000015473

The polarization model will allow for a degree of polarization provided by the lunar model with respect to the input phase angle. It is provided as an optional extra output.

2.7.4 DoLP spectral dependency

The DoLP appears to be spectrally-dependent as well, with an increased spectral dependence for higher phase angles.

Figure 17: Modelled DoLP for all wavelengths (negative phase angle)

DoLP retrievals in between 1088 instrument wavelengths, i.e. the central wavelength of a sensor spectral band, are interpolated linearly.

3 Model uncertainties

3.1 Initial concepts

The Guide to the Expression of Uncertainty in Measurement (BIPM, 2008), and its supplements provide guidance on how to express, determine, combine and propagate uncertainty. The GUM and its supplements are maintained by the JCGM (Joint Committee for Guides in Metrology), a joint committee of all the relevant standards organisations and the International Bureau of Weights and Measures, the BIPM. The documents describe both the "Law of Propagation of Uncertainty" (hereafter, LPU) and Monte Carlo methods of uncertainty propagation.

The LPU propagates standard uncertainties for the input quantities through a locally-linear first-order Taylor series expansion of the measurement function to obtain the standard uncertainty associated with the measurand. Higher order approximations can be applied if necessary.

Monte Carlo methods approximate the input probability distributions by finite sets of random draws from those distributions and propagate the sets of input values through the measurement function to obtain a set of output values regarded as random draws from the probability distribution of the measurand. The output values are then analysed statistically, for example to obtain expectation values, standard deviations and error covariances. The measurement function in this case need not be linear nor written algebraically. Steps such as inverse retrievals and iterative processes can be addressed in this way. The input probability distributions can be as complex as needed, and can include distributions for digitised quantities, which are very common in EO, where signals are digitised for on-board recording and transmission to ground.

Monte Carlo methods can provide information about the shape of the output probability distribution for the measurand, deal better with highly non-linear measurement functions and with more complex probability distributions, and can be the only option for models that cannot be written algebraically (including for iteration). However, they are computationally more expensive, which is an important consideration with the very high data volumes of EO.

3.2 Fitting

In this project there are several fitting processes. First for each night's data, a straight line is fitted to the raw data for the Langley plot method; second the lunar model (separated into linear and nonlinear components) is fitted to the TOA lunar irradiance values obtained for each night; and third the spectral data are fitted to a spectral model. The process is further complicated by iteration both at the Langley plot stage to consider the lunar phase change during the Langley plot, and with the lunar model fitting outlier removal process.

We can consider uncertainties at several levels of complexity in fitting processes:

- At the simplest level, the fitting is done with an unweighted least squares approach (or non-linear, iterative, equivalent, such as the Levenberg-Marquardt method), taking no account of uncertainties in the fit itself.
- At the next simplest level, we may use uncertainties to weight the data going into the fitting process. This could be a weighted-least-squares fit (where the residual is divided by the uncertainty before being squared and summed), or, more simply, by introducing a cut-off (outlier removal)
- In a more robust method, the covariance of the input quantities and uncertainties in the X_i and Y_i would be considered in the fitting process. Here the full input quantity covariance would be included in the fit process. (e.g. methods such as generalised least squares – if the

uncertainties are in one quantity only, or orthogonal distance regression – if the uncertainties are in both axes).

- In the most robust method a measurement model is developed that includes error quantities for the input measurements and fits the values of those errors as well as the desired model parameters as part of the fit process. This is known as "errors in variables" fitting.

Note that each of these methods would not only provide a different uncertainty associated with the fitting but would also give a different value for the fit. When uncertainties and error covariance are taken into account in the fit process, then the fit will be different. To understand this, consider the simplest example of the difference between a simple mean and a weighted mean. If some measured values have much larger uncertainties than others, then in a simple mean the fit will be closer to these, in a weighted mean, it would be closer to those points with smaller uncertainties.

With the more robust approaches, the covariance of the fit parameters (the uncertainty associated with each parameter and the covariance between any pairs of parameters) would be determined "automatically" – in the sense that it can be easily calculated from the available information and would normally be calculated as part of the analysis. With the simpler approaches there is a need to calculate the uncertainty separately.

For a simple linear regression, the uncertainty can be calculated analytically. Alternatively, and more easily for complex multi-stage or iterative regressions, Monte Carlo methods can provide an uncertainty. Whether analytical or Monte Carlo approaches are used, care must be taken in interpreting the uncertainty determined – the determined uncertainty will be based on the assumptions. It assumes that the model being fitted is consistent with the data.

3.3 Approach to uncertainty analysis for this project

Within this project our approach is to use the simplest form of fitting and to apply Monte Carlo analysis to estimate uncertainties. We also indicate how, in later work, we can take some of the input quantity uncertainties into account in the fitting itself.

The Monte Carlo analysis is fed with random errors, based on the knowledge of uncertainties provided with the measurements. In practice, every measurement will be slightly adjusted with a random error which lies within the uncertainty interval.

We currently use an estimate of the typical uncertainty associated with the fit of the individual Langley plots based on statistical analysis of the range of uncertainties observed, as described below in section 3.4. The input for the Monte Carlo analysis is perturbated at least 1000 times and thus 1000 lunar models are calculated from the perturbated input.

3.4 Uncertainties in the Langley Plot intercept

The Langley Plot fits a straight line to the logarithm of signal as a function of airmass. As discussed in our report [AD2], the uncertainty associated with airmass is considered negligible. The uncertainty associated with the signal (corrected for instrument temperature effects and for lunar phase changes during the Langley[1], as well as for sun-moon and moon-Earth distances) is dominated by the noise in the measurement.

[1] The correction for lunar phase changes during the Langley is performed by iterating the Langley plot and lunar model fitting several times.

This measurement noise was estimated in the D4 report [AD2] from the statistics of the triplet (each observation being three observations made very close together in time).

Table 4 Table given in D4 (there Table 28) with additional line for combined standard uncertainty

Term	Uncertainty [%]					
	1640nm	1020nm	870nm	675nm	500nm	440nm
D(λ, t)	0.07	0.05	0.02	0.01	0.03	0.04
$F_T(\lambda)$	0.0027	0.13	0.18	0.17	0.15	0.053
$F_T(\lambda)$	0.002	0.037	0.001	0.002	0.003	0.003
K_{dist}	0	0	0	0	0	0
$A(t_{ref},\lambda)/A(t,\lambda)$	0.006	0.006	0.006	0.006	0.006	0.006
+0 (aerosol's diurnal cycle)	0	0	0	0	0	0
Combined standard uncertainty	0.070	0.144	0.181	0.170	0.153	0.067

The residuals observed in the initial model fit however indicate that the uncertainty associated with individual Langley plots using these values is an underestimation.

In D4 we discussed that this could be in part because of changes in aerosol (and other atmospheric) properties during the Langley. We described there that at least some of such a variation may not be visible in the Langley analysis itself as the curve would "still look linear", however, since we do see variations in the Langleys that have a clear "shape" to them, we also allow for the possibility that these atmospheric variations may also cause random or semi-random effects in the Langley fitting.

Table 5: Uncertainty associated with atmospheric effects during the Langley [AD2]

	Uncertainty in Vo [%]							
	1640nm	1020nm	870nm	675nm	500nm	440nm	380nm	340nm
Aerosol	0.2	0.2	0.3	0.3	0.5	0.5	0.5	0.7
Other	0.17	0.25	0.01	0.12	0.17	0.19	0.31	0.5
Total	0.37	0.45	0.31	0.42	0.67	0.69	0.81	1.2

It is also reasonable to assume that using a standard deviation of the triplets, which shows instrument stability over a very short period of time, underestimate the uncertainty associated with the stability of the instrument for the duration of the Langley.

3.4.1 Fitting the Langley

The original fitting for this project used a simple least squares analysis fit that does not take into account the uncertainty associated with each data point, nor provides an uncertainty associated with the intercept.

Based on the residuals observed indicating a potential underestimation of the uncertainty associated with the Langleys , we performed a more rigorous analysis where each data point was given the same relative uncertainty taken from the standard deviation of the triplets. (See APPENDIX A for more

information about how this fit was done and APPENDIX C for how logs were dealt with). The fit routine we used then also calculated the uncertainty associated with the intercept and the χ^2 value of the fit. Where the observed χ^2 was smaller than the expected χ^2, the intercept uncertainty was accepted as given. Where the observed χ^2 was larger than the expected χ^2, relative uncertainty on each data point was increased by small increments until the χ^2 test was passed.

3.4.2 Example Langley statistics

When performing the fit and applying the χ^2 test, very few of the Langley plots passed using the original uncertainty on the input parameters. This is as expected from the observed residuals in the model fit. For those that failed, uncertainty on input parameters was increased incrementally until the test was passed and uncertainty associated with the y-intercept, $\ln(V_0)$ was determined. A small selection required a small increase in uncertainty for each data point, and a few had high uncertainty indicating that the fit should be considered for removal from the dataset or have very low weighting in the final model

Example Langley plots are shown below

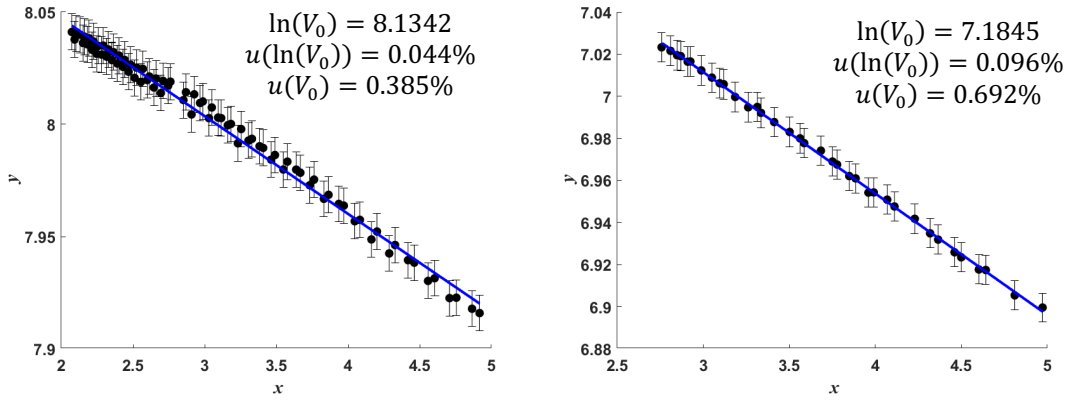

Figure 18: Langley plots which pass χ^2

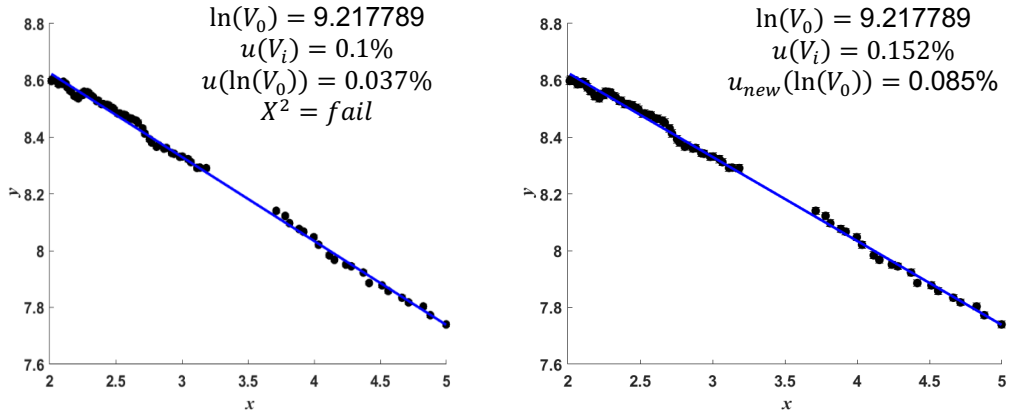

Figure 19: Langley before increase uncertainty (left) and after (right)

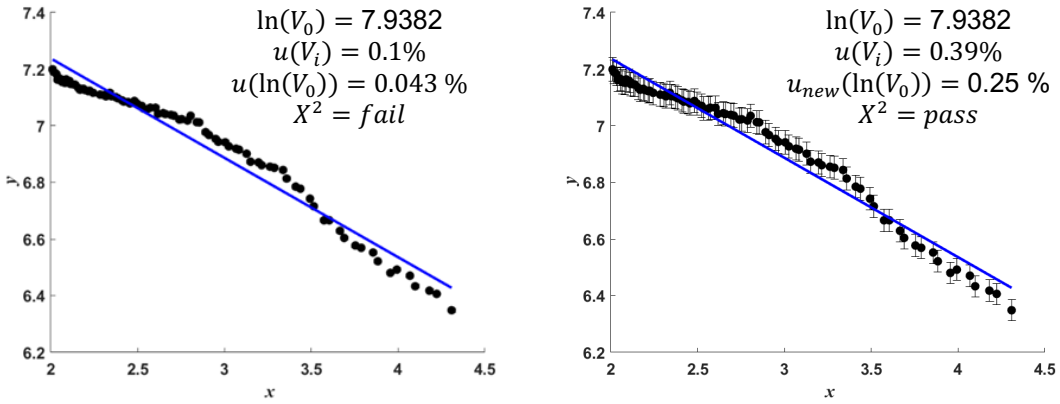

Figure 20: Langley before increase uncertainty (left) and after (right)

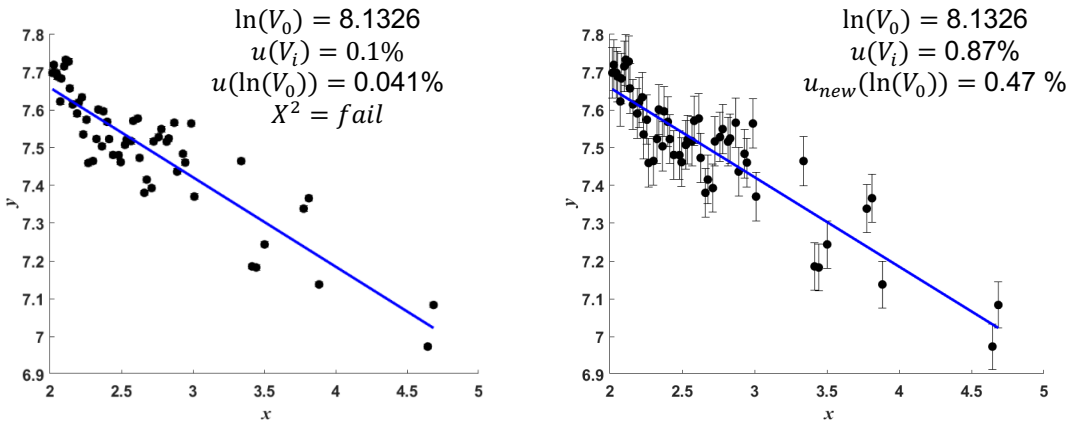

Figure 21: Langley before increase uncertainty (left) and after (right)

Using the values of $u(\ln[V_0])$ an and the $u_{new}(\ln[V_0])$ where appropriate we plotted a histogram of the uncertainty associated with the y-intercept of the Langley plots for each wavelength, and from this determined a 'typical' uncertainty that would be used in the Monte Carlo uncertainty analysis input parameters. Ideally, we should carry forward the individual uncertainty determined for each Langley and weight each value of V_0 determined from individual Langley plots in the model fit, and this is something to be considered in future improvements of the model.

Table 6: Estimated uncertainty in y-intercept of Langley plots

	440 nm	500 nm	675 nm	870 nm	1020 nm	1640 nm
$\boldsymbol{u(ln[V_0])}$	0.35%	0.25%	0.16%	0.18%	0.47%	0.61%

The initial estimates for uncertainty in $ln\ (V_0\ )$ presented in Table 6 are the 'typical' uncertainties determined by statistical analysis of the range of intercept uncertainties for the set of Langley plots in this analysis. These estimates are obtained before considering the later outlier removal process implemented by UVa which iteratively removes any 3-sigma outliers during an initial model fit process.

A large proportion of Langley plots with high uncertainties in the fit are removed during the model fit outlier removal, however some are not, and this highlights the need to consider this fit uncertainty in the next iteration of the model.

After removal of these outliers identified in the model fit process we find that the typical uncertainty associated with the linear fit of the Langleys reduces to those values presented in

. As a first approximation these values are used in this iteration of the model, although more ideally we would consider the uncertainty in each individual Langley plot and weight each data point in model fit accordingly. We also set an upper limit whereby any Langley plots with uncertainty 5 times higher than the typical uncertainty are currently removed from the dataset.

Table 7: Estimated uncertainty in the y-intercept of the Langley plots, after removal of those data points filtered by the model fit outlier removal process

	440 nm	500 nm	675 nm	870 nm	1020 nm	1640 nm
$\boldsymbol{u(ln[V_0])}$	0.21%	0.16%	0.13%	0.12%	0.12%	0.21%

3.5 Fitting the lunar model

The lunar model fit is described in section 2. This is a multistep process where the linear part of the model is fit for each band, then outliers are removed, then the non-linear part is fit (all bands simultaneously), there is further outlier removal and finally the linear part is fit again. The whole multistep process is itself iterated.

To understand the uncertainties associated with the method, we use Monte Carlo Uncertainty Analysis (MCUA). The MCUA process is based on a measurement model. In this case we treat the input irradiance values (the TOA irradiance values for each night obtained by the Langley Plot process) as

$$E_{i,\lambda} = E_{i,\lambda}^{\text{True}} \times \left(1 + R_{i,\lambda}\right)(1 + S_\lambda)(1 + C) \qquad (6)$$

Here:

$E_{i,\lambda}^{\text{True}}$ is the nominal "true" value for the TOA irradiance in spectral band λ for the ith observation

$R_{i,\lambda}$ is the error in the observation in spectral band λ for the ith observation due to random effects, expressed in relative terms, e.g. as a percentage of the true value

S_λ is the error in the observation that is common for all measurements in this band, expressed in relative terms, e.g. as a percentage of the true value

C is the error in the observation that is common for all measurements in all bands, expressed in relative terms, e.g. as a percentage of the true value

The error values are unknown; but are draws from a probability distribution with a standard deviation given by the relative uncertainty associated with this effect and with an expectation value (central value) of zero.

$R_{i,\lambda}$ takes a different value for every observation. This comes from random processes relating to the measurement of the TOA irradiance for a particular night. These include instrument noise, instrument temperature changes and atmospheric changes – and relates to the relative uncertainty in the Langley Plot intercept that is estimated above [section 0].

S_λ takes the same value for every observation for a single spectral band. This comes from effects that are common for that band – and mostly that is from the NPL calibration of the instrument. Any uncertainty associated with the NPL calibration is "fixed" into that calibration and applied to all measurements.

C takes the same value for every single observation in all spectral bands. This comes from effects in the NPL calibration that are wavelength independent, e.g. from a distance offset on an instrument alignment.

3.5.1 The uncertainties associated with systematic errors

The uncertainties associated with the systematic errors S_λ and C originate from the calibration of the CIMEL photometer at NPL and calculated from the uncertainty analysis outlined in deliverable D4 [AD4], and are described in the previous section.

The uncertainties associated with the calibration were separated into 4 categories:

a. Fully independent effects (e.g. noise) where the error varies statistically from observation to observation (e.g. is different at different distances and for the different methods)
b. Fully common effects (e.g. instrument alignment) where the error is (almost) identical for all measurements with all sources at all distances
c. FEL399 effects (e.g. its calibration) where the error is common to all methods that use FEL399
d. Method common effects where the error is common to the measurements at different distances with this method but which is different for other methods

Here we identify that categories a and d vary from spectral band to spectral bad, and so will make up the S_λ input parameters for the MCUA and, categories b and d will be largely systematic for all channels and so make up C. These values are presented in Table 8.

Note that in D4 [AD4], we considered one spectral band at a time, and were combining results from multiple calibration measurements. Therefore, these categories do not transfer perfectly from that process to here (where band-to-band error correlation is more important). However, there is sufficient overlap to use those categories as a starting point. Future activity could propagate band-correlation separately.

Table 8 : Systematic uncertainties per band S_λ and to all measurements C

	440 nm	500 nm	675 nm	870 nm	1020 nm	1640 nm
S_λ	0.77%	0.73%	0.55%	0.63%	0.31%	0.31%
C	1.1%	1.1%	1.1%	1.1%	1.1%	1.1%

3.5.2 The uncertainties associated with random errors

The uncertainty associated with random errors is given by the uncertainty in the Langley Plot intercepts. Above (Section 3.4) we showed that the uncertainty in the intercept could range from 0.1 % to 0.61 % however this is reduced once we consider the outlier removal in the model fit.

Because the uncertainty associated with systematic effects is, by definition, causing a common error to all the observation values being fitted by the lunar model, the variation between the measured data points and the model must be explained either by inaccuracies in the model form, or by the uncertainties associated with random effects.

We can use an initial estimate of the model parameters, calculated without taking uncertainty into account, to compute the residuals – the difference between the model and the measured value. These differences should fall within the uncertainties. To test this we plotted a histogram of these residuals divided by their associated uncertainties. i.e. we have

$$\Delta_{residual} = \frac{(V_{meas} - V_{model})}{u(V_{meas})} \qquad (7)$$

Where, V_{meas} and V_{model} are the irradiance values for the measurement and model respectively and $u(V_{\mathrm{meas}})$ is the absolute uncertainty (i.e. the relative uncertainty in percent multiplied by the value $u_{\mathrm{rel}}(V_{\mathrm{meas}}) \times V_{\mathrm{meas}}$) associated with that measurement.

When the model is well fitted by the measurements, and when the measurement uncertainty is correctly estimated, this [either form!] will be a Gaussian[2] distribution with a mean of zero and standard deviation of 1. If the standard deviation is very much less than 1, then uncertainties are overestimated, if it is very much greater than 1, then uncertainties are underestimated and if the shape is not Gaussian, then the model may not be a good fit to the data, or there are significant outliers.

When we do this calculation with the initial uncertainties we get the following plots :

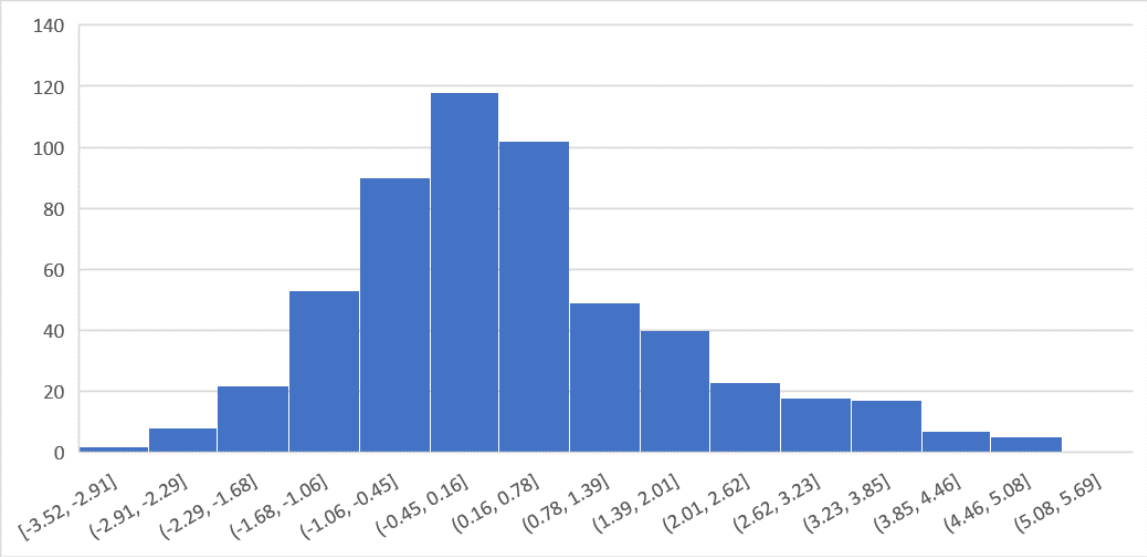

Figure 22: Relative residual histogram 1088+933 model before filtering

[2] For very small numbers of data points it will be a T-distribution.

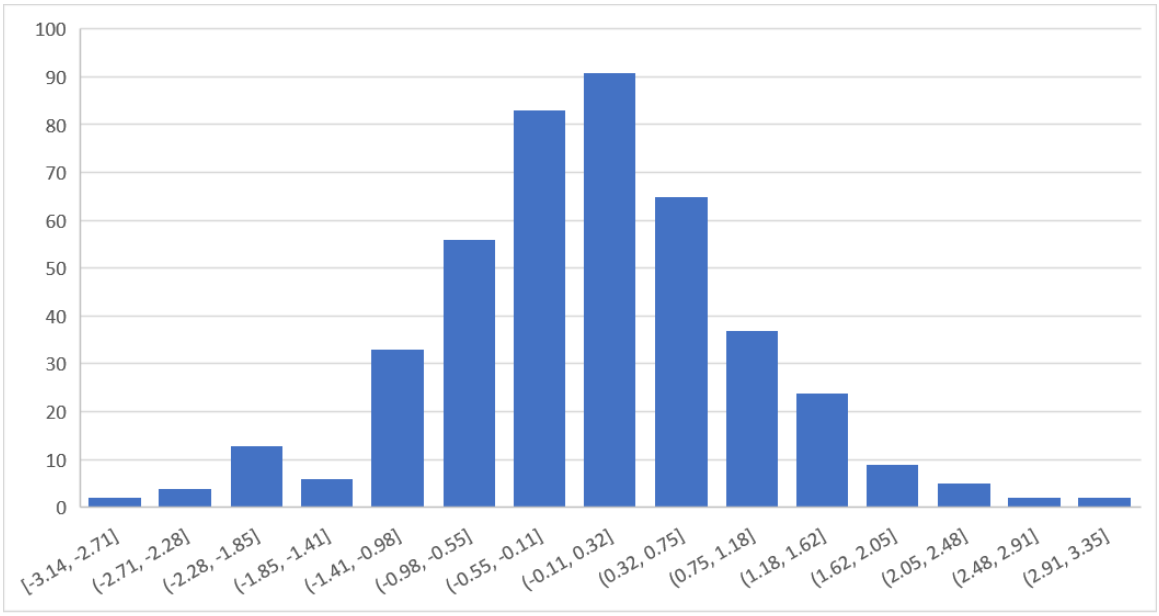

Figure 23: Relative residual histogram 1088+933 model after filtering

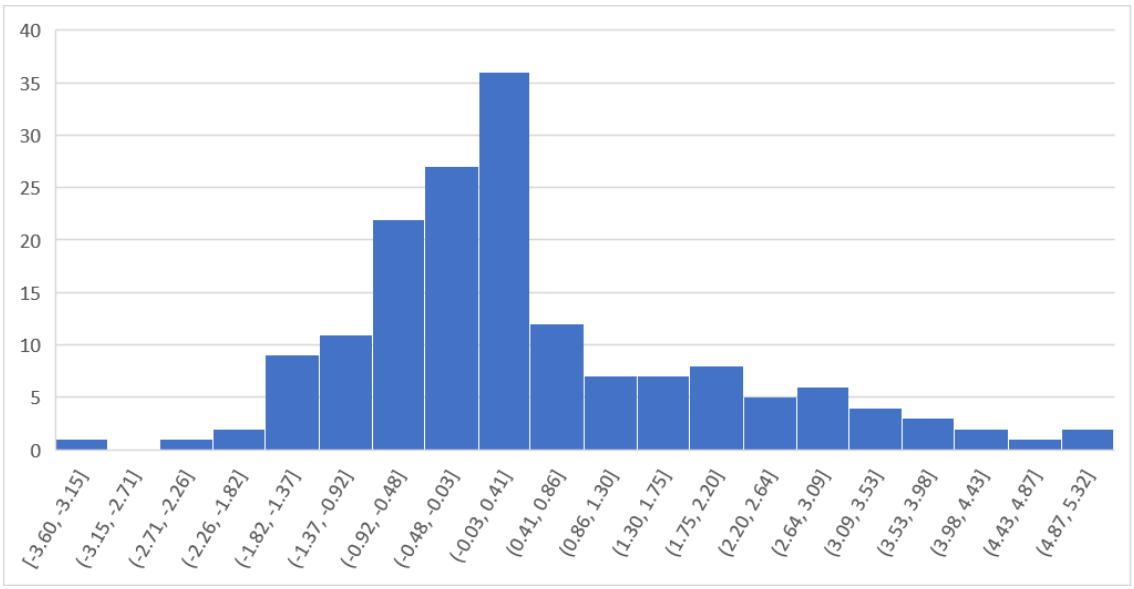

Figure 24: Relative residual histogram 1088 model before filtering

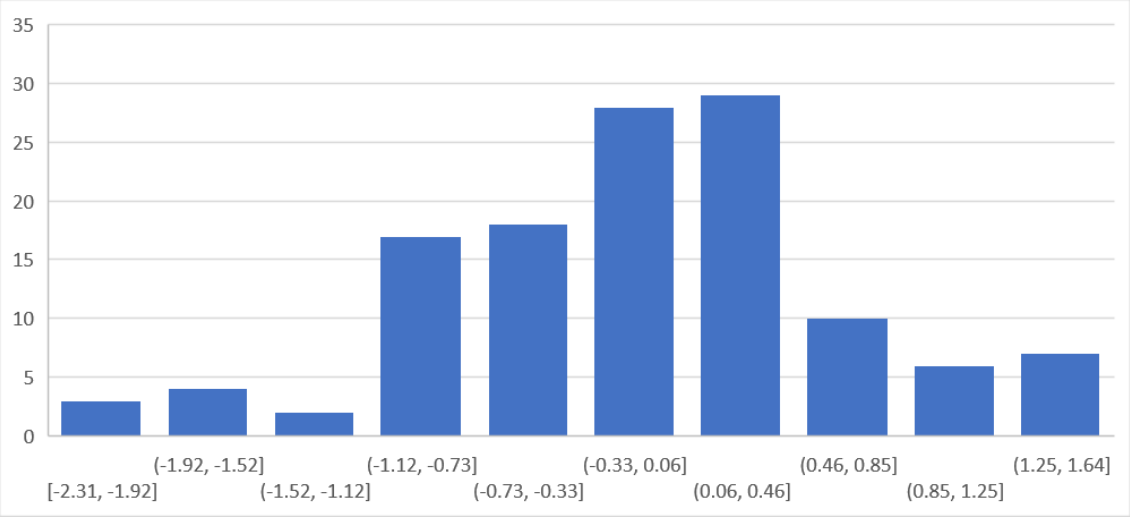

Figure 25: Relative residual histogram 1088 model after filtering

The plots show that these residuals are more gaussian shaped after the filtering process. It is also quite clear that more samples (555 for 1088+933 as opposed to 166 for 1088) results in a more standard gaussian distribution.

Statistics in the next table show that after filtering, the averages are already close to zero for both models and the standard deviation is close to one, after the filtering process. We hope to be able to improve the number, when we updated the model to include individual uncertainties for every measurement.

Table 9 : Statistics associated with model relative residuals

model	average unfiltered	stdev unfiltered	average filtered	stdev filtered
1088+933	0.298	1.475	-0.026	0.951
1088	0.386	1.535	0.011	0.927

3.5.3 Performing the Monte Carlo Uncertainty Analysis

The MCUA is performed only for the final iterative step. Here, we run the fit routine 1000 times. For each iteration we create a single value of the error C drawn randomly from a Gaussian distribution with a central value 0 and a standard deviation equal to the uncertainty associated with C. We draw 6 values S_λ, each corresponding to a different spectral band, and we draw as many values of $R_{i,\lambda}$ as are needed – the number of spectral bands multiplied by the number of observations.

Conceptually, we alter the input values by these errors, perform the fit and then obtain a model based on those errors. We then repeat this 1000 times to give 1000 different models. Thus, in pseudo code we have:

```
For k = 1 to 1000
        Choose C from a random Gaussian of width u(C)
        Choose S_lambda for each band from the appropriate random Gaussians
        For i = 1 to the number of observations, N
                Choose a set of R_i for each band from Gaussians
                Calculate irradiance from Equation (above)
```

Fit the model, get fit parameters set i
Loop observations
Loop Monte Carlo run

Practically, we need to modify this somewhat to account for the fact that the fit occurs on the logarithm of reflectance rather than the irradiance, and is for the final iteration of the final, post outlier removal, linear fit.

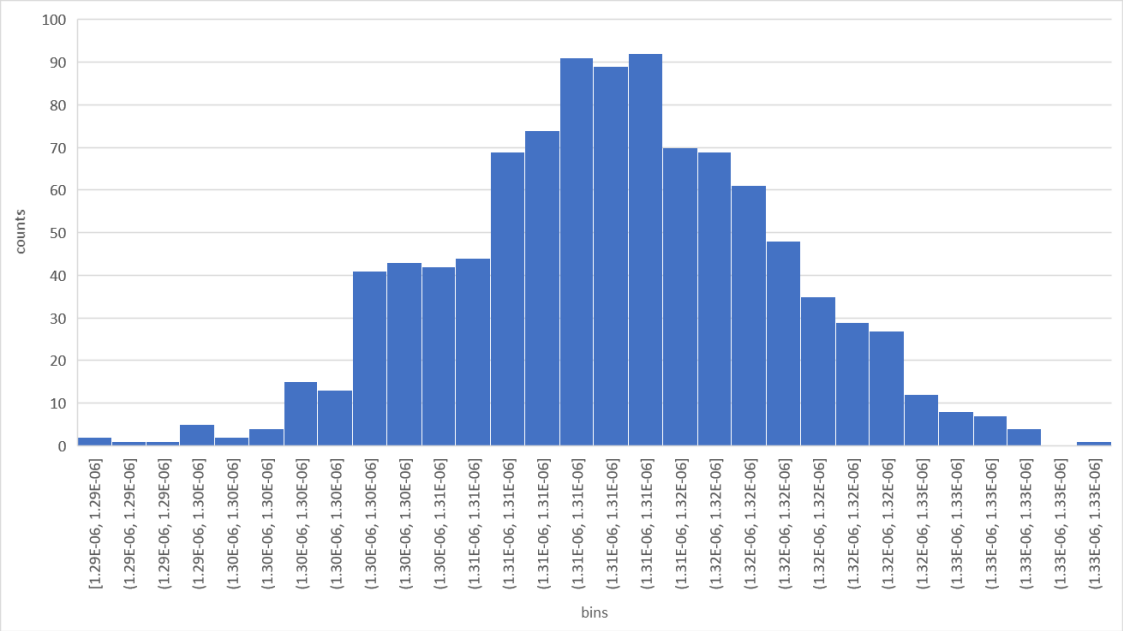

Figure 26: example of perturbated input irradiance for one measurement

For one iteration, all measurements of all bands are perturbated with a factor (%) calculated from the above scheme - 1000 times a new model is fit.

3.5.4 Calculating the uncertainty and covariance of the fit parameters

At the end of the MCUA process we have 1000 versions of the model that differ from one another in a way that is consistent with the uncertainties and covariances of the input quantities. We can use these to estimate the uncertainty associated with the model. The first step is to estimate the uncertainty associated with the fit parameters and the covariance between pairs of fit parameters.

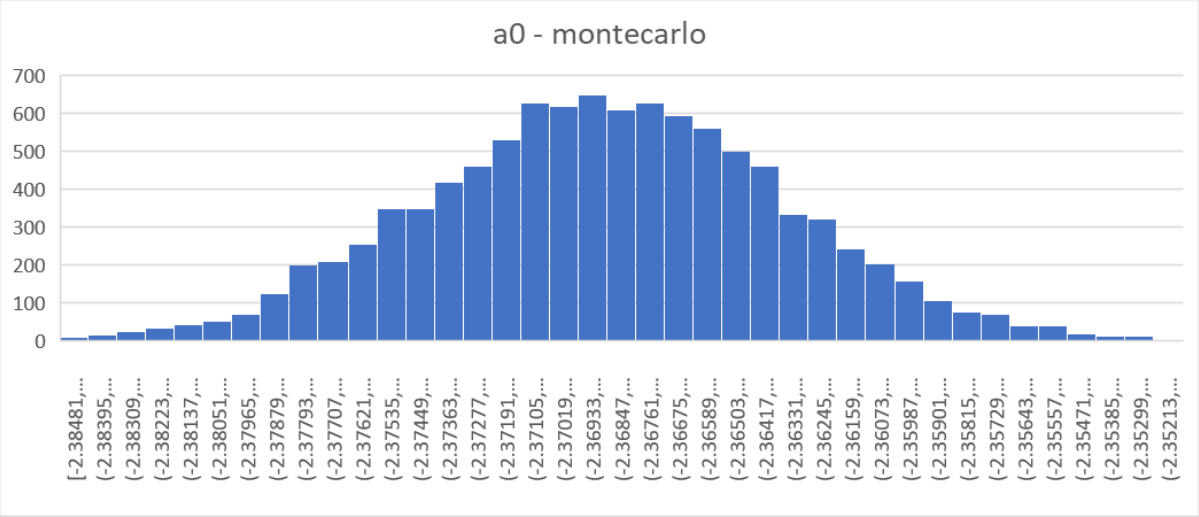

Figure 27 : monte carlo output for coefficient a0

This is done statistically. The uncertainty is determined by taking the sample standard deviation of the 1000 instances of each fit parameter. We get for the first band

wl[nm]	**a0**	**a1**	**a2**	**a3**	**b1**	**b2**	**b3**
440	-2.76443	-0.77946	-0.28446	-0.02657	0.051998	0.011877	-0.00584
wl[nm]	**c1**	**c2**	**c3**	**c4**	**d1**	**d2**	**d3**
440	0.00144	-8.4E-05	0.001911	0.001031	1.111408	2E+132	0.003075
	p1	**p2**	**p3**	**p4**			
all	1.448495	18.99534	10.77744	9.002714			

Figure 28: Statistics for model 440 band (mean fit parameter from MCUA, standard deviation of the 1000 estimates, and the standard deviation expressed as a percentage of the mean value).

It is also valuable to estimate the correlation coefficient of the different fit parameters for a single spectral band, or for the different spectral band for a given fit parameter. This is calculated using the standard formula for the sample Pearson correlation coefficient.

	a0	a1	a2	a3	b1	b2	b3	c1	c2	c3	c4	d1	d2	d3	p1	p2	p3	p4
a0	1.000000	-0.539161	0.530155	-0.518675	0.070539	-0.123045	0.149257	0.031141	-0.007576	-0.029292	-0.057731	0.282807	-0.283089	0.248621	-0.404896	-0.404829	-0.319940	0.319177
a1	-	1.000000	-0.995087	0.982249	-0.129463	0.226003	-0.275749	-0.058253	0.034145	0.046046	0.113490	-0.515960	0.516468	-0.454136	0.731448	0.731092	0.579855	-0.578564
a2	-	-	1.000000	-0.995748	0.137411	-0.242317	0.298290	0.060667	-0.039522	-0.046223	-0.127477	0.500355	-0.500858	0.436304	-0.714102	-0.714017	-0.562116	0.560846
a3	-	-	-	1.000000	-0.145271	0.259627	-0.323479	-0.064996	0.042775	0.048682	0.145481	-0.484153	0.484647	-0.419807	0.694384	0.694501	0.543619	-0.542380
b1	-	-	-	-	1.000000	-0.886272	0.745499	0.009393	0.079067	0.029071	-0.060304	0.067467	-0.067538	0.063356	-0.093377	-0.093412	-0.071492	0.071398
b2	-	-	-	-	-	1.000000	-0.959775	0.002928	0.003774	0.066227	0.147046	-0.121846	0.121954	-0.104609	0.164763	0.164198	0.136932	-0.136656
b3	-	-	-	-	-	-	1.000000	0.007164	-0.047092	-0.112758	-0.210064	0.145869	-0.145997	0.118802	-0.199157	-0.198383	-0.167309	0.166918
c1	-	-	-	-	-	-	-	1.000000	-0.402845	-0.053920	-0.019270	0.058748	-0.058770	0.055017	-0.051686	-0.050823	-0.050337	0.050590
c2	-	-	-	-	-	-	-	-	1.000000	0.037962	-0.062008	-0.029820	0.029820	0.001789	0.019704	0.019199	0.023283	-0.023477
c3	-	-	-	-	-	-	-	-	-	1.000000	-0.388492	-0.038111	0.038130	-0.036052	0.040598	0.039759	0.039443	-0.039466
c4	-	-	-	-	-	-	-	-	-	-	1.000000	-0.004544	0.004616	-0.009300	0.047189	0.049170	0.011108	-0.010816
d1	-	-	-	-	-	-	-	-	-	-	-	1.000000	-0.999999	0.627920	-0.717032	-0.690887	-0.894020	0.898366
d2	-	-	-	-	-	-	-	-	-	-	-	-	1.000000	-0.628000	0.717719	0.691612	0.894047	-0.898389
d3	-	-	-	-	-	-	-	-	-	-	-	-	-	1.000000	-0.584447	-0.567397	-0.689432	0.689495
p1	-	-	-	-	-	-	-	-	-	-	-	-	-	-	1.000000	0.998949	0.796552	-0.794968
p2	-	-	-	-	-	-	-	-	-	-	-	-	-	-	-	1.000000	0.769137	-0.767422
p3	-	-	-	-	-	-	-	-	-	-	-	-	-	-	-	-	1.000000	-0.999948
p4	-	-	-	-	-	-	-	-	-	-	-	-	-	-	-	-	-	1.000000

Figure 29: Correlation matrix 440 nm coefficients

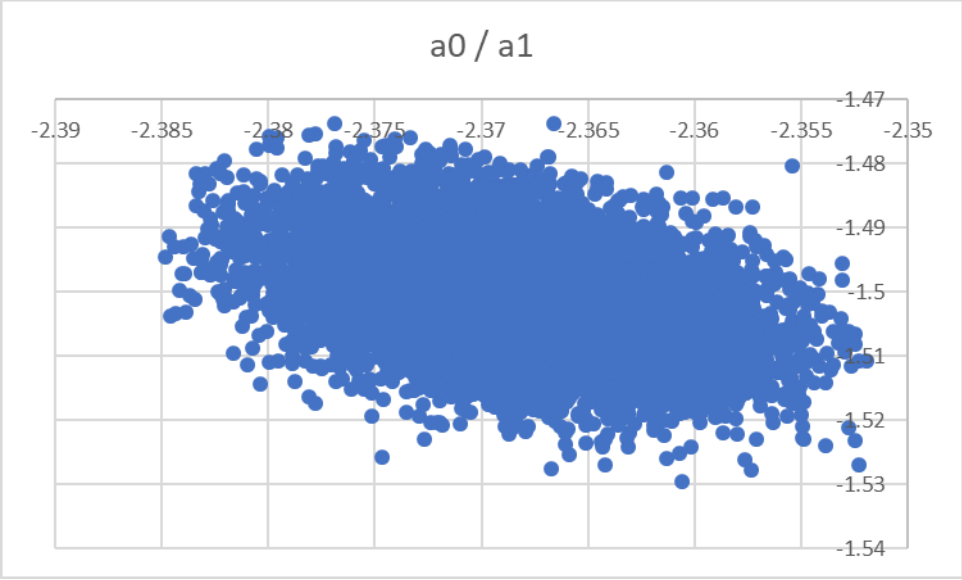

Figure 30: Low correlation between a0 and a1

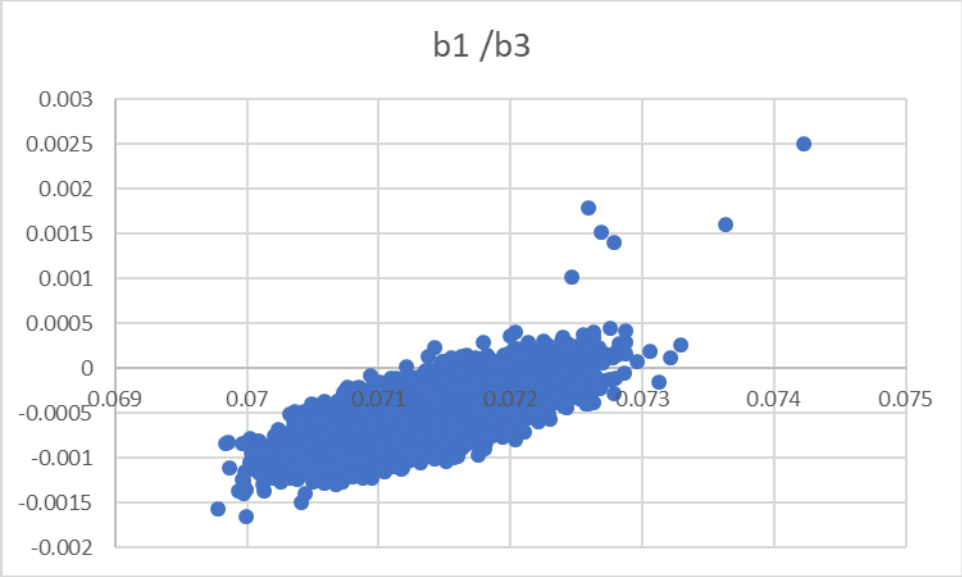

Figure 31: High correlation of 0.74 between b1 and b3 band

Any high correlation (>0.5) suggests that the model is not well defined – i.e. that you could add something to one and compensate by removing it from the other. Such models can be hard to fit, so this may indicate the value of removing one of those parameters. Permanent evaluation of the MCUA results is part of the future work, when measurements become available. These results might ultimately result in an updated formulation of the model. Currently we don't draw any conclusions on these results, as individual measurement uncertainties are not yet included, as well as the number of 1088 measurements is limited to 2 years.

A covariance matrix is calculated for the fit parameters by having on-diagonal terms equal to the square of the absolute uncertainty associated with that fit parameter and the off-diagonal terms equal to $u(a_i, a_j) = u(a_i)(a_j)r(a_i, a_j)$.

	a0	a1	a2	a3	b1	b2	b3	c1	c2	c3	c4	d1	d2	d3	p1	p2	p3	p4
a0	3.430E-05	-3.642E-05	3.874E-05	-1.279E-05	1.947E-07	-5.325E-07	2.351E-07	4.567E-09	-1.126E-09	-5.044E-09	-9.766E-09	1.475E-01	-1.476E-01	3.070E-07	-1.432E-04	-1.279E-04	-1.524E-05	2.011E-08
a1	-	1.330E-04	-1.432E-04	4.770E-05	-7.039E-07	1.926E-06	-8.552E-07	-1.683E-08	9.996E-09	1.562E-08	3.781E-08	-5.299E-01	5.305E-01	-1.104E-06	5.094E-04	4.549E-04	5.440E-05	-7.179E-08
a2	-	-	1.557E-04	-5.231E-05	8.082E-07	-2.234E-06	1.001E-06	1.896E-08	-1.252E-08	-1.696E-08	-4.594E-08	5.559E-01	-5.565E-01	1.148E-06	-5.380E-04	-4.806E-04	-5.705E-05	7.528E-08
a3	-	-	-	1.773E-05	-2.884E-07	8.079E-07	-3.663E-07	-6.854E-09	4.572E-09	6.028E-09	1.770E-08	-1.815E-01	1.817E-01	-3.727E-07	1.766E-04	1.578E-04	1.862E-05	-2.457E-08
b1	-	-	-	-	2.222E-07	-3.087E-07	9.450E-08	1.109E-10	9.461E-10	4.030E-10	-8.211E-10	2.832E-03	-2.835E-03	6.297E-09	-2.658E-06	-2.375E-06	-2.741E-07	3.621E-10
b2	-	-	-	-	-	5.461E-07	-1.907E-07	5.419E-11	7.078E-11	1.439E-09	3.139E-09	-8.018E-03	8.026E-03	-1.630E-08	7.352E-06	6.546E-06	8.231E-07	-1.086E-09
b3	-	-	-	-	-	-	7.230E-08	4.824E-11	-3.214E-10	-8.915E-10	-1.632E-09	3.493E-03	-3.496E-03	6.735E-09	-3.234E-06	-2.878E-06	-3.660E-07	4.829E-10
c1	-	-	-	-	-	-	-	6.272E-10	-2.561E-10	-3.970E-11	-1.394E-11	1.310E-04	-1.311E-04	2.905E-10	-7.816E-08	-6.866E-08	-1.025E-08	1.363E-11
c2	-	-	-	-	-	-	-	-	6.443E-10	2.833E-11	-4.546E-11	-6.740E-05	6.741E-05	9.575E-12	3.020E-08	2.629E-08	4.807E-09	-6.411E-12
c3	-	-	-	-	-	-	-	-	-	8.646E-10	-3.300E-10	-9.979E-05	9.984E-05	-2.235E-10	7.208E-08	6.307E-08	9.434E-09	-1.248E-11
c4	-	-	-	-	-	-	-	-	-	-	8.343E-10	-1.169E-05	1.187E-05	-5.664E-11	8.231E-08	7.662E-08	2.610E-09	-3.361E-12
d1	-	-	-	-	-	-	-	-	-	-	-	7.930E+03	-7.930E+03	1.179E-02	-3.856E+00	-3.319E+00	-6.476E-01	8.606E-04
d2	-	-	-	-	-	-	-	-	-	-	-	-	7.931E+03	-1.179E-02	3.859E+00	3.323E+00	6.476E-01	-8.607E-04
d3	-	-	-	-	-	-	-	-	-	-	-	-	-	4.445E-08	-7.440E-06	-6.453E-06	-1.182E-06	1.564E-09
p1	-	-	-	-	-	-	-	-	-	-	-	-	-	-	3.646E-03	3.254E-03	3.913E-04	-5.164E-07
p2	-	-	-	-	-	-	-	-	-	-	-	-	-	-	-	2.910E-03	3.375E-04	-4.454E-07
p3	-	-	-	-	-	-	-	-	-	-	-	-	-	-	-	-	6.617E-05	-8.751E-08
p4	-	-	-	-	-	-	-	-	-	-	-	-	-	-	-	-	-	1.157E-10

Figure 32: covariance matrix for all model coefficients of 440nm

3.5.5 Calculating the uncertainty associated with the model

The full model combines these spectral band observations with a spectral fit based on lunar rock reflectance measurements. In a later phase of this programme (future project) we intend to use hyperspectral observations of the moon to provide intermediate model values. For now, we are using existing data used in the GIRO model [RD2].

In the current iteration of the model we assume (erroneously, but in the absence of other information) that there is no uncertainty associated with the observations used in the spectral interpolation, nor with the interpolation process itself. Instead we will simply propagate our uncertainties by continuing the MCUA, creating 1000 hyperspectral moon models and considering the variability. Uncertainty associated with the spectral observations and interpolation will be included in later phases of the project.

The irradiance is calculated for every input measurement used in the coefficient regression. The results per input measurement is the 1000x applied model. The irradiance is calculated using the instrument response curves.

An example of this output is plotted, showing a normal like distribution (Figure 33). Such plot could be produced for every measurement and hence the mean and standard deviation is calculated.

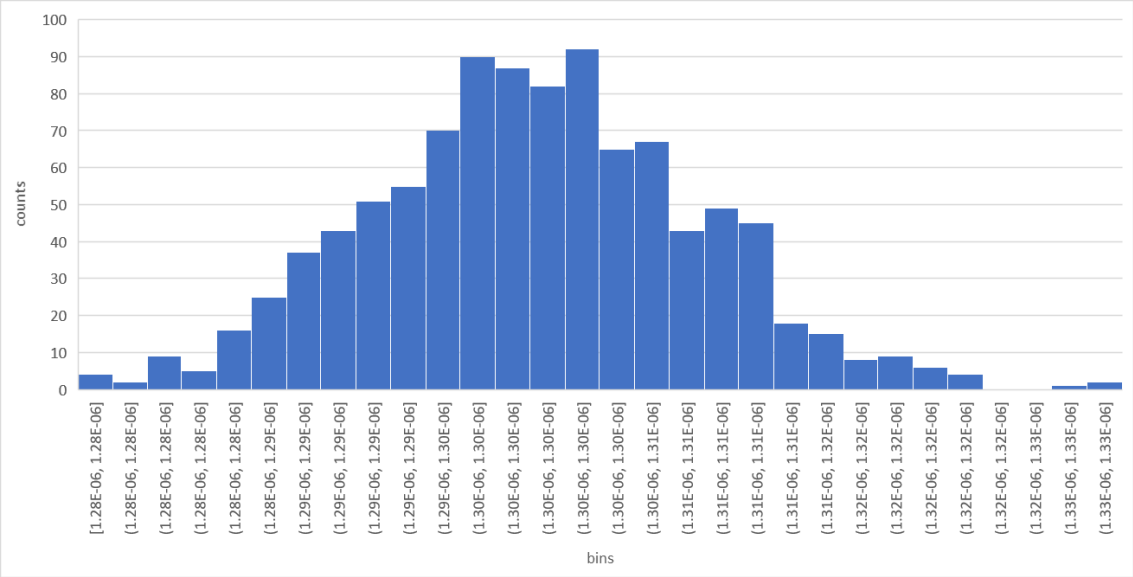

Figure 33: Distribution of the results for one input measurement of band 440nm

The extended relative uncertainty is calculated from the standard deviation of the output distributions.

$$u(E_{i,\lambda}) = k * \frac{s(E_{i,\lambda})}{E_{i,\lambda}} \qquad (8)$$

$E_{i,\lambda}$ is the measured irradiance value, before any perturbation is applied, $u(E_{i,\lambda})$ is the relative uncertainty, *k* is the factor applied to obtain the required confidence interval for a normal distribution, $s(E_{i,\lambda})$ is the standard deviation of all models results for this measurement.

From the results, as shown in Figure 34, the uncertainty level is quite stable over phase angle, except for angles close to outside the model phase angle limits [-90.0:-2.0-2.0:90.0]. In the summarizing plots, the uncertainty values have been averaged per 5° phase angle.

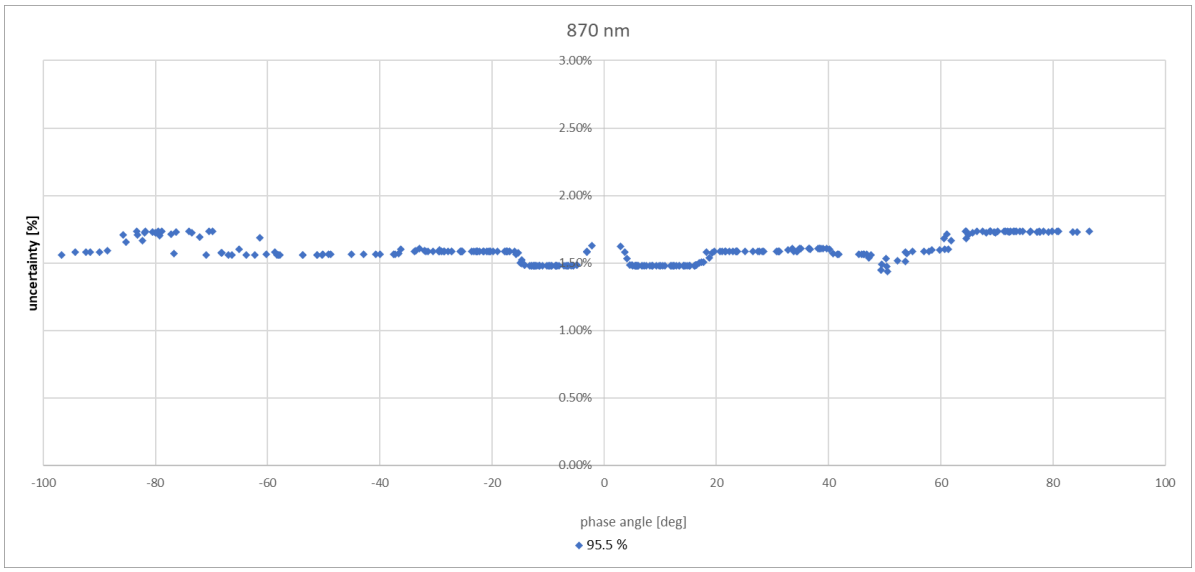

Figure 34: 95.5% uncertainty band 870nm

Figure 35 up to Figure 40 show the uncertainty levels for all bands, averaged per 5 degrees. Uncertainty levels at 95.5 % (*k* = 2.0) and 99.7 % (*k* = 3.0) confidence level are shown, as well as the mean $E_{i,\lambda}$ obtained averaged over 1000 results. This is not the irradiance from the "root" model output.

When looking at the plots, one can see that for the 95.5% confidence interval, all bands perform well below 2 % except for band 440 nm.

For the 99.7 % confidence level, all bands perform approximately at 2.5 % uncertainty, except for the 400 nm and 500 nm bands, which are slightly above.

The model and its uncertainties here are provided for the 1088 instrument. It must be noted that the Langley plots with the high uncertainty in the intercept are currently included in the fit. This is due to the fact that there are not enough data points after excluding these to satisfactorily fit the model. In the next phases of the project, it is intended that these will be removed as described in section 3.4.

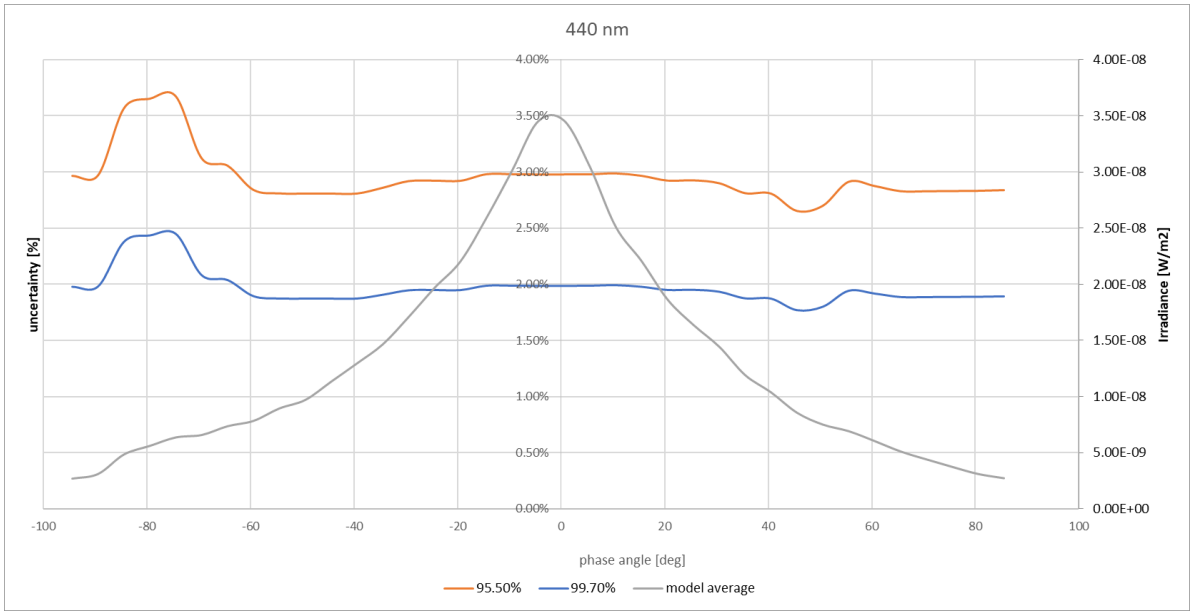

Figure 35: Uncertainty levels for the 440nm band

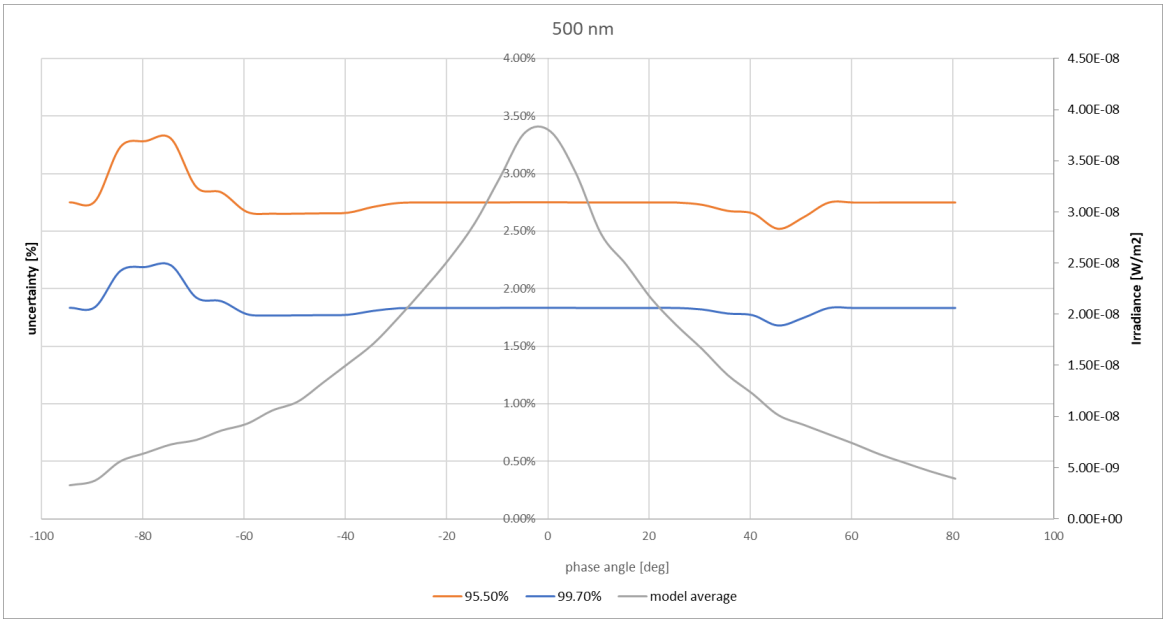

Figure 36: Uncertainty levels for the 500nm band

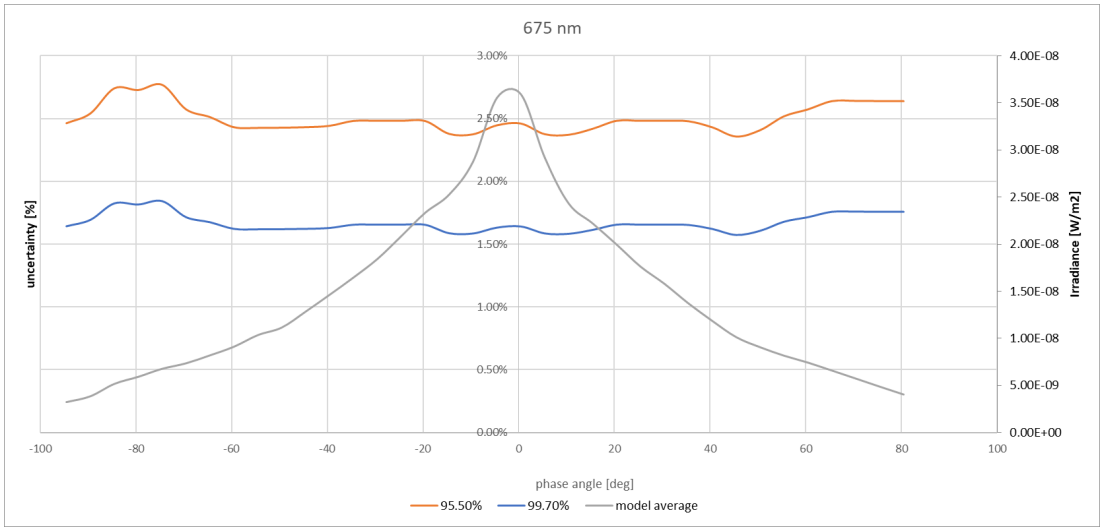

Figure 37: Uncertainty levels for the 675nm band

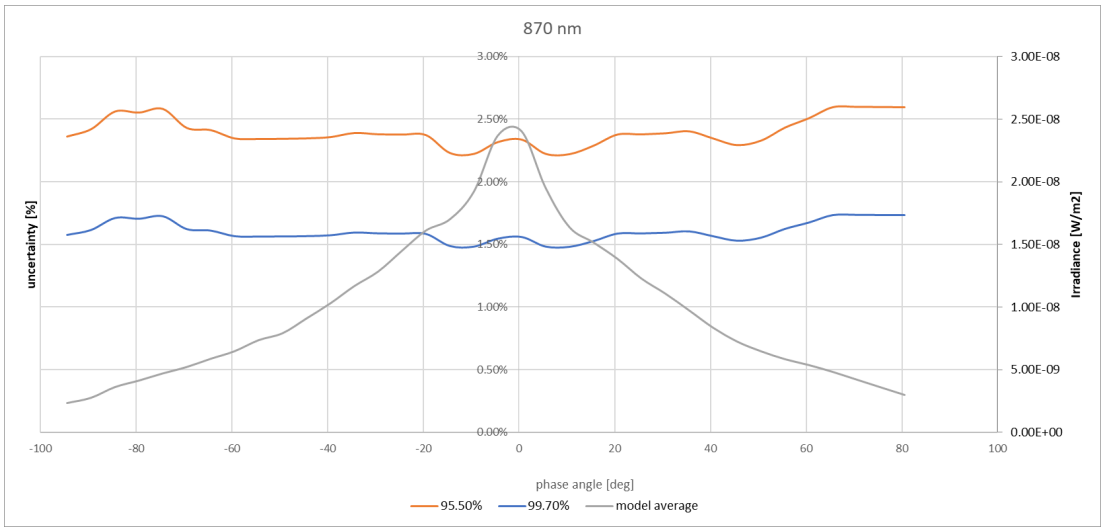

Figure 38: Uncertainty levels for the 870nm band

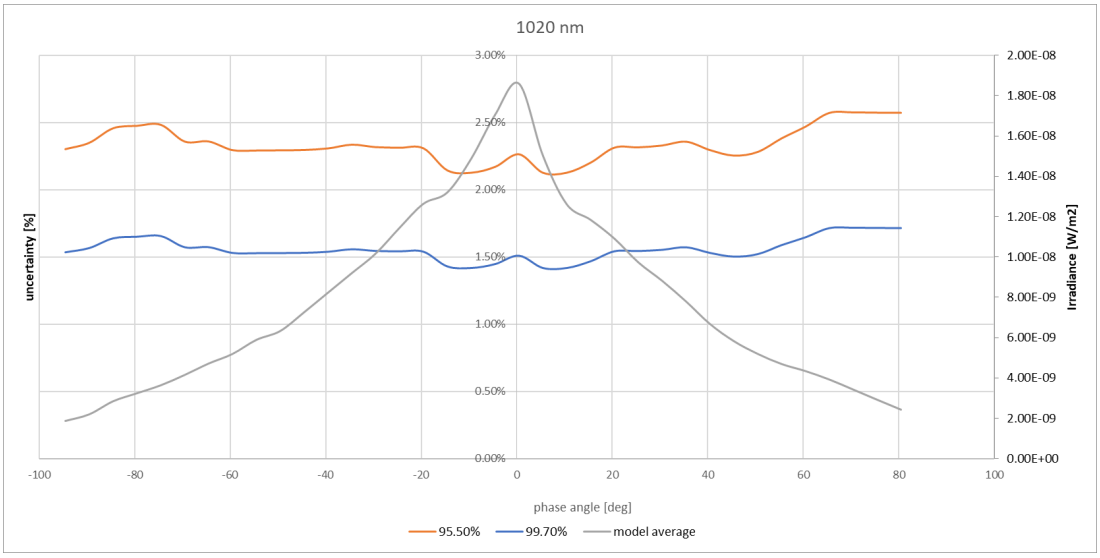

Figure 39: Uncertainty levels for the 1020nm band

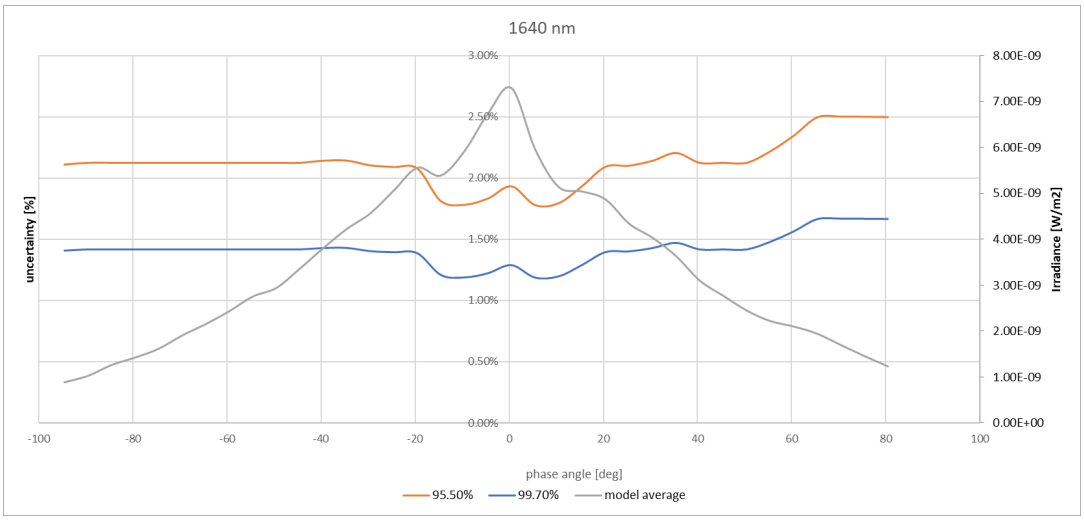

Figure 40: Uncertainty levels for the 1640nm band

3.5.6 Evolution of model uncertainties with number of measurements

To get a clear understanding of the evolution of the uncertainty levels with respect to the amount of used measurements, the MCA is performed on both the 1088 measurements only and the 1088+933 measurements. It appears that in general the uncertainty level stays the same for both regressions.

There is a slight difference of around 0.2% with large positive phase angles and about 0.1% for specific low phase angles. This can be interpreted as very low differences. This has to be re-evaluated during the process of model iterations, when more 1088 measurements become available. Applying the uncertainty budgets from the 1088 instrument on the 933 instrument is not good practice and should be avoided.

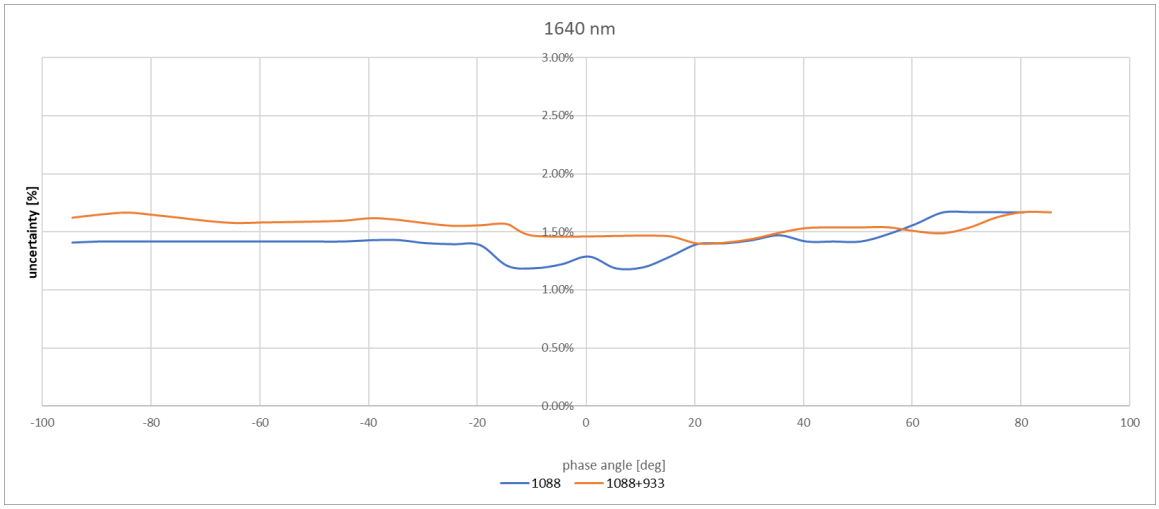

Figure 41: Uncertainty level for both 1088 and 1088+933 model regression

4 Conclusions

This report has described the process involved in fitting a lunar-reflectance model to the measured Langley plot intercepts. The lunar-reflectance has been calculated using both the 1088 instrument specified, purchased, calibrated and installed as part of this project, and the 933 instrument that has been used for a longer period. A polarization model has also been established, based on the polarized observations from the 1088 instrument. Spectral interpolation has used the existing ROLO model.

With the current uncertainty budget analysis, a full system uncertainty characterization has been performed. Based on the lab calibrations, uncertainties for the different measurement stages are identified :

- Systematic uncertainties (common to all)
- Uncertainties linked to instrument spectral band
- Uncertainties linked to every measurements separately.

A method has been derived to estimate the uncertainty for every measurement, based on the Langley fitting process. This algorithm has been plugged into the measurement facilities at the Izaña institute and will provide in the future a measurement specific uncertainty. In the next iteration, these individual uncertainties will also be plugged into the Monte-Carlo analysis, allowing for a more accurate characterization of the model uncertainties.

With the current setup, using the estimated ‘average’ Langley uncertainties for every measurement (Table 7) the outcome of the Monte-Carlo analysis show a reasonably flat uncertainty value for all model spectral bands. The 95 % confidence interval shows an uncertainty level of 2 % or less for all bands. The 99 % gave uncertainties between 2.5% to 3% depending on the spectral band. We believe that, with increasing number of measurements from the 1088 instrument and more accurate uncertainty estimates, the levels of uncertainty will slightly decrease and flatten out. This is however to be confirmed in the next iteration.

In summary, future work to improve the model will include:

- Obtaining additional measurements (6 years of data are required to cover the full range of different lunar cycles)
- Improved spectral observations from the Pandora instruments used to develop spectral interpolation
- Improved handling of negative polarization
- Provision of an uncertainty associated with each Langley plot and a weighted fit that takes into account those uncertainties
- Uncertainties associated with spectral interpolation

5 Acknowledgements

Special thanks goes to Tom Stone for having several fruitful discussions on the existing ROLO model and its possible adaptations. Without his help and legacy, this project would not have reached its current level of success.

Also thanks to EUMETSAT for providing the GIRO model, to be used in the comparison with the new developed model. A subset of the measurements from this project will be contributed to the GLOD, the GIRO Lunar Observations Database, to be used in future inter-comparisons.

APPENDIX A – Dealing with logs in the uncertainty analysis

It is not possible to apply the Law of Propagation of Uncertainties to a logarithm directly. The logarithm and exponential functions are highly nonlinear and in this case we do not have dimensionless quantities. If we just take a logarithm of the uncertainty, we get the wrong uncertainty for the logarithm of the value. Instead we calculate the uncertainty associated with the logarithm numerically.

To understand this, we consider a simple quantity, y, which is the natural logarithm of the measured signal V, thus

$$y = \ln(V)$$

Therefore, we can write

$$V = \exp(y).$$

To evaluate an uncertainty, we perturb the measured signal, V by a small perturbation, δV.

$$V + \delta V = \exp(y + \delta y)$$

Taking a logarithm of both sides we get

$$\ln(V + \delta V) = (y + \delta y)$$

And rearranging:

$$\delta y = \ln(V + \delta V) - y.$$

We make δV equal to the uncertainty associated with the signal, and use the result δy as the uncertainty associated with the y-axis model process.

To check for symmetry, try $\delta V = +u(V)$ and $\delta V = -u(V)$. For highly non-linear functions this may not be symmetrical.

APPENDIX B – Fitting a straight line with uncertainty information

In this case we consider fitting a straight line to measured data points with some associated uncertainties which may differ from point to point. The method described here calculates both a slope and intercept for the straight line and their associated uncertainties and covariance using the uncertainties associated with the y-values. There is assumed to be no uncertainty associated with the x-values.

The calculation of the slope and offset is as follows:

The weights[3] are defined as

$$w_i = \frac{1}{u(y_i)} \tag{0.1}$$

where $u(y_i)$ is the uncertainty associated with the measured value y_i at the set value x_i.

The reference values are given by

$$x_0 = \frac{\sum_{i=1}^{N} w_i^2 x_i}{\sum_{i=1}^{N} w_i^2}, \qquad y_0 = \frac{\sum_{i=1}^{N} w_i^2 y_i}{\sum_{i=1}^{N} w_i^2}. \tag{0.2}$$

The slope is then calculated as

$$b = \frac{\sum_{i=1}^{N} w_i^2 (x_i - x_0)(y_i - y_0)}{\sum_{i=1}^{N} w_i^2 (x_i - x_0)^2} \tag{0.3}$$

and the intercept as

$$a = y_0 - bx_0 . \tag{0.4}$$

The variance (squared uncertainty) and covariance associated with the slope and intercept are given by

$$\begin{aligned} u^2(b) &= \frac{1}{\sum_{i=1}^{N} w_i^2 (x_i - x_0)^2}, \\ u^2(a) &= \frac{1}{\sum_{i=1}^{N} w_i^2} + \frac{x_0^2}{\sum_{i=1}^{N} w_i^2 (x_i - x_0)^2}, \\ u(a,b) &= \frac{-x_0}{\sum_{i=1}^{N} w_i^2 (x_i - x_0)^2}. \end{aligned} \tag{0.5}$$

APPENDIX C – Producing a covariance matrix for the input observations

To do a full uncertainty analysis and a fit that fully takes into account the covariance at the lunar model fitting, we would need a covariance matrix for the input observations. We have an input observation model of

$$E_{i,\lambda} = E_{i,\lambda}^{\text{True}} \times (1 + R_{i,\lambda})(1 + S_\lambda)(1 + C)$$

A covariance matrix for the full set of observations (all bands, all actual measurements) would have as its diagonal the uncertainty associated with a single observation, squared, i.e.

[3] Because this term is squared in the subsequent equation, the actual weight is inversely proportional to the square of the uncertainty.

$$u^2(E_{i,\lambda}) = \left(E_{i,\lambda}^{\text{meas}}\right)^2 \times \left[u_{\text{rel}}^2(R_{i,\lambda}) + u_{\text{rel}}^2(S_\lambda) + u_{\text{rel}}^2(C)\right]$$

The covariance for two measurements on the same band would be

$$u(E_{i,\lambda j}, E_{i,\lambda k}) = \left(E_{i,\lambda j}^{\text{meas}}\right)\left(E_{i,\lambda k}^{\text{meas}}\right) \times \left[u_{\text{rel}}^2(S_\lambda) + u_{\text{rel}}^2(C)\right]$$

And the covariance for two measurements in different bands would be

$$u(E_{i,\lambda j}, E_{i,\lambda k}) = \left(E_{ij,\lambda j}^{\text{meas}}\right)\left(E_{ik,\lambda k}^{\text{meas}}\right) \times \left[u_{\text{rel}}^2(C)\right]$$

In practice because we have to do our model in terms of log reflectance, this model would first have to be propagated to reflectance (straightforward, analytic) and then to log reflectance (numerically).